LARGE SCALE INTEGRATION OF ELECTRIC VEHICLES INTO THE POWER GRID AND ITS POTENTIAL EFFECTS ON POWER SYSTEM RELIABILITY

by

Mingzhi Zhang

A Thesis Submitted in

Partial Fulfillment of the

Requirements for the Degree of

Master of Science

in Engineering

at

The University of Wisconsin-Milwaukee

May 2017

ABSTRACT

LARGE SCALE INTEGRATION OF ELECTRIC VEHICLES INTO THE POWER GRID AND ITS POTENTIAL EFFECTS ON POWER SYSTEM RELIABILITY

by

Mingzhi Zhang

The University of Wisconsin-Milwaukee, 2017
Under the Supervision of Professor Lingfeng Wang

In this thesis, the potential effects of large scale integration of electric vehicles into the power grid are discussed in both the beneficial and detrimental aspects. The literature review gives a comprehensive introduction about the existing smart charging algorithms. According to the system structure and market mechanism, the smart charging algorithms can be divided into centralized and distributed method. With the knowledge of driving patterns and charging characteristics of electric vehicles, both the centralized and decentralized smart charging algorithms are studied in this research.

Based on the smart charging pricing and sequential price update mechanism, a multi-agent based distributed smart charging algorithm is used in this research to flatten the load curve and therefore mitigate the potential detrimental effects caused by uncoordinated charging. Each EV agent has some extent of intelligence to solve its own charging scheduling problem. The optimization method used in this research is the binary hybrid GSA-PSO algorithm, which combines the merits of particle swarm optimization (PSO) and gravitational search algorithm (GSA), and has very good exploration and exploitation abilities. A V2G enabled centralized smart charging algorithm is also introduced in this thesis, each EV can earn revenues by discharging power into the grid. The dominant search matrix is used to

resolve the "curse of dimensionality" problem existing in the centralized optimization problems. Numerical case studies show both the distributed and V2G enabled smart charging algorithms can effectively transfer the charging load from the peak load period to the load valley hours.

Because of the limited integration ratio of electric vehicles, most power system reliability methods do not evaluate the charging load of EVs separately in their analytical procedures. However, with a fast increasing integration level, the potential effects of large scale integration of EVs on the power system reliability should be comprehensively evaluated. The effects of EV charging on power system reliability in the planning phase is analyzed in this research based on the RBTS. The results show the uncontrolled charging will deteriorate the reliability level while the smart charging can effectively decrease the detrimental effect. The potential application of aggregated EV providing operating reserve to the grid as a kind of ancillary service is also discussed, and the related effects on power system reliability in operating phase are calculated using the modified PJM method. The case study shows the unit commitment risk of the system can decrease to a very low level with the additional operating reserve capacity provided by aggregated EVs, which can not only improve the system's reliability level but also save the cost.

TABLE OF CONTENTS

LIST OF TABLES

LIST OF FIGURES

ACKNOWLEDGMENTS

I would like to thank my supervisor Professor Lingfeng Wang for his help, guidance and encouragement during my study in UWM. Professor Wang's professionalism, patience and dedication to the research have a profound influence on my career path. His humor, wisdom and attitudes also enlightened me about the essence of life. I fell very proud and grateful to have a chance to do research under his supervision.

I would like to thank Professor Chunlin Guo from North China Electric Power University for the patient guidance and training in the early stage of my research. I would also like to thank Professor David Yu and Professor Xiao Qin for acting as the committee members.

I would like to thank senior students Jun Tan and Yingmeng Xiang for so many times' discussions, their experiences and suggestions are valuable for this research work.

Finally, I would like to thank my parents, Haoqun Zhang and Weihua Gao, without their continuing encouragement and support, it's hard to imagine I could go as far as now on the academic path.

Chapter 1

Introduction

1.1 Research background

Large-scale electric vehicles and plug-in hybrid vehicles (EVs and PHEVs) integration into the power and transportation system has been envisioned for the first half of the 21st century. Sales number of EVs and PHEVs begin to grow rapidly after 2015 and is estimated to reach 7 million per year by 2020, and 100 million by 2050 [1], According to the statistical data from Electric Drive Transportation Association(EDTA), 2.99% of the U.S. automotive market is contributed by EVs and PHEVs by 2016, there are 580,569 plug-in vehicles sold in US since 2010 [2].

There are mainly three different types of electric vehicles: battery electric vehicle (BEV), hybrid electric vehicle (HEV), and plug-in-electric vehicle (PHEV) [3]. Battery electric Vehicles (BEVs) use battery-powered motor, they run exclusively on electric power via on-board batteries, which can be charged by plugging into the electric power system through different methods. EV use electric motor and therefore do not use gasoline at all. The Nissan LEAF, Fiat 500e, Chevrolet Bolt and Tesla Series fall into this category. Hybrid Electric Vehicles (HEVs) can use both electric power and gasoline, the battery on board is charged with regenerative braking and

internal combustion engine. Unlike BEVs and PHEVs, HEVs can not be plugged into the grid for charging. Because this research focus on the interaction between vehicles and power system, HEVs are not considered in this research. Plug-in Hybrid Electric Vehicles (PHEVs) also can use both gasoline and electric power stored in on board battery. Different with the HEVs, the battery can be charged by plugging into power grid. Because PHEVs can run with both gasoline and electricity, it's suit for long distances driving if the charging station's availability is unknown.The Chevy Volt, Toyota Prius, BMW i8, Audi A3 E-Tron fall into this category. In this thesis, the electric vehicles (EVs) mean battery electric vehicle (BEV) or plug-in-electric vehicle (PHEV).

The large scale integration of EVs into the power grid can lead to potential issues including power unbalance, power losses increase, voltage deviation, etc [4]. However with properly coordinated control, it can greatly minimize those adverse impacts. The flexibility of EVs in both time and spatial scale can also be resources, which makes it capable for taking multi-roles in the power system. It can be load (charging), energy storage system (ESS), and power source (discharging). Compared with the conventional thermal generating units, large amounts aggregated vehicle batteries nearly do not have startup cost or shutdown cost at all when discharging power to the grid [5], which make it suitable for responding the fluctuations in power system caused by high ratio integration of renewable energy.

1.2 Benefits of large scale integration of EVs

1.2.1 Economic Benefits

The economic benefits of EV can be observed from EV owners and the power grids perspectives. For the EV owners, the costs are comparatively less than the traditional internal combustion engine (ICE) because of the high efficient electric

motors. The typical efficiency of ICE is 15-18%, however the efficiency of EV can be as high as 60-70% [6]. In recent years, the developments of battery technologies have already greatly improved the life time, performance indexes and economics metrics of batteries [7]. However, the prices of EV now are still much higher than ICE vehicles. In fact, the price can be significantly reduced by mass production and clean energy trading policies. Some companies like Tesla are making progress on this direction.

Meantime, the integration of electric vehicles into the power grid can bring many potential opportunities, such as the vehicle-to-grid (V2G) technology could be a solution for the stochastic, uncertain issues of renewable energy [8]. The concept of V2G shows EV owners can earn profits by transferring their EV battery from load to energy storage systems, even distributed generation sources with proper market and control mechanism. Kim et al. [9] showed EV's characteristics of fast dynamic response can be used to enable buildings to compensate for the high-frequency components of load demand variations, and its effective in reducing the frequency deviations and required reserve capacity. Aghaei et al. [10] discussed the importance of plug-in vehicles and their problems and investigated their potential applications as mobile storages for the integration of RESs and demand response programs. Sioshansi and Denholm [11] showed an EV fleet can reduce the cost of power system by $200-$300 per year per vehicle. By using EVs, it can improve residential customers' competitive positions in demand response programs and can help decreasing the negative impacts of EVs' charging.

1.2.2 Environmental Benefits

The large scale integration of EVs is recognized as one of the most promising solutions to air pollution and carbon dioxide emission. The impacts of massive adoption of PHEVs on greenhouse gas (GHG) emissions reduction was investigated in [12] for Los Angeles. PHEVs' effects on GHG emissions are dependent on type and

scale of generation sources, adoption rate, and charging behavior. Donateo et al. [13] put forward a method that use measured data of electric consumption to quantify its emissions of CO2 and pollution, by using Italian electricity production mix of each recharging event and the emissions factors of the Italian power plants, this research showed the EVs have advantages in CO2, carbon monoxide, nitrogen oxide emissions.

Well-to-wheels (WTW) analysis on electric vehicles (EVs) have been used extensively to evaluate the potential energy and environmental effects, Ke et al. [14] collected up-to-date data concerning the electricity generation mix, fuel transport, end-of-pipe controls, real-world fuel economy and emissions, the WTW energy consumption and CO_2 and air pollutant emissions for various light-duty passenger vehicle technologies currently (2015) and in the mid-term future (2030) are estimated. The results showed the WTW CO_2 emissions by EVs should approach to 100 gkm^{-1} by 2030 due to the increased integration ratio of renewable clean electricity, even lower than that of hybrid electric vehicles.

The environmental impacts of electric cars depend on the source of electricity. The increasing integration ratio of renewable energy can promote further reduction of pollutant emissions. For the city of Athens during 2012-2020, by using a penetration scenario of 10% biodiesel, 10% natural gas and 10% electricity to the energy mix of the vehicle fleet, Nanaki et al. [16] showed by using biodiesel, natural gas and EVs can decrease the CO_2 emissions by 21.1% compared to 2012's level and NO_x by 57.2%.

1.3 Adverse impacts of large scale integration of EVs into the power grid

Although with all the merits introduced in last section, the large scale integration of EVs into the existing power system may cause a lot problems, the analysis of

potential adverse impacts and specific solutions are critical to not only the safe and reliable operation of power system but also the long term development of EVs.

1.3.1 Increased peak load demand

Various studies have been done about the impact of EVs' charging on grid peak load demand. The potential peak power and energy demand by the integration of electric vehicles are examined for the city of Perth, Western Australia in [17]. This research showed the uncoordinated charging with a high EV penetration ratio can cause the peak demands surpassing the generating system capacity on average days. Smart charging and time-of-use (TOU) tariff plan can significantly reduce the peak demand, so the optimization of charging and discharging behaviors of EVs is based on given variations in electricity spot prices, user preferences and driving patterns, then it can avoids the extra generation capacity expansion [18].

1.3.2 Power quality issues

A stable power grid is critical for the reliable power supply. The characteristics of EV charging loads are different from the traditional household or industrial loads, therefore, the effects of EV charging loads on grid power quality [19, 20, 21, 22, 23] have been extensively analyzed.

Gmez and Morcos [19] investigated the impacts of harmonic distortion caused by EV chargers on distribution system, especially on transformers. This proposed method can be used to determine the optimal charging time according to the base load, ambient temperature, and time. This study also showed that uncoordinated direct charge can be detrimental to the transformer life, especially under high temperature and large load scenarios. A probabilistic harmonic simulation method are put forward in [21] to study the power quality impacts of EVs. The random and stochastic characteristics of the vehicles, such as charging begin time, charging dura-

tion, and locations are taken into the Monte-Carlo simulation process. A harmonic current source model was used to model the harmonic characteristics of EV charger, the results showed that Level 1 charger may cause the rise of neutral to earth voltage, which could lead to stray voltage incidents.

A similar stochastic modeling and simulation technique are used in [22] to analyze the impacts of EVs' charging demands on distribution network. Different from the probabilistic method, the feeder daily load models, electric vehicle start charging time, and battery state of charge used are derived from actual measurements and survey data. A modified IEEE 13-bus test system and a 25-bus Taiwan Power Company (TPC) distribution system were used for numerical analysis, the Monte Carlo simulations and roulette wheel selection concept were used to simulate the uncertainties of SOC and charging time. This study showed the stochastic approach can present significant risk information by determining many under-voltages and over-currents cases.

The impacts of EV charging on residential low voltage distribution network in Malaysia are analyzed in [23] in aspects of voltage profile, voltage unbalance and transformer thermal limit. The results showed that distribution networks can safely operate at 10% penetration ratio with uncontrolled charging, and smart charging can increase the penetration ratio to 60% without adverse impact on distribution system voltage. Razeghi et al. [20] focused on the impacts of plug-in hybrid electric vehicles on a residential transformer using both stochastic and empirical analysis, the hot spot temperature and loss of life of transformer are calculated based on a thermal model. The results showed the transformer might fail due to excessive temperatures with Level 2 charging. By proper design and using smart charging control, the negative effects on the life time of transformer can be greatly mitigated.

1.4 Smart charging and its potential effects on power system reliability

As discussed in last section, large scale integration of EVs may cause lots of problems like increased peak load, power quality issues, power losses and transformer loss of life. Increasing the investment on the update of existing distribution network is one option, however, a more economical choice is to reduce the bad effect with smart charging control, it can greatly minimize those adverse impacts. Kiviluoma and Meibom [24] calculated that smart charging can save 227 Euro per year per vehicle compared with immediate uncontrolled charging. Most of the benefits come from smart timing of charging and providing reserves. Kara et al. [25] estimated the potential benefits of smart charging by collecting data from more than 2000 non-residential electric vehicle supply equipments (EVSEs) in Northern California for the year of 2013. The results showed that the smart charging control of aggregated electric vehicles can decrease the contribution to system peak load by approximately 37%.

Smart charging change the traditional role of EV as passive load in the distribution network, instead it seeks to achieve active control of EVs for certain objectives, such as reduce the peak load, minimize the generation costs or operation losses. System costs and peak demand can be further reduced by the integration of renewable energy.

Controlled smart charging can decrease the system costs and peak demand compared with uncontrolled charging, meantime the plug-in electric vehicles' characteristics of controlled charging rate providing a fast and economic way to balance the supply and load demand. Compared with the method of using fast-responding natural gas turbines, this method can potentially reduce the operation costs and the construction of new power plants [26]. Meantime, the V2G technology allows aggregated EV to play the roles of energy storage systems and distributed generators in

the system, so it can therefore provide different kinds of ancillary services [27, 28] (frequency regulation, spinning reserve, demand side response), which are valuable for power system with high ratio of renewable energy integration.

The effects of smart charging on power system reliability become a hot topic in recent years. Liu et al. [29] used a bidirectional charging control algorithm and combined the EV charging with the generation system adequacy. The results showed the smart charging control can effectively improve power generation adequacy. Xu and Chuang [30, 31] used the well-being analysis framework to analyze the power system generating system reliability with electric vehicles charging considered. However, because of the relatively low integration ratio now, the research in this area is still lacking.

1.5 Research objectives and thesis structure

This research focus on analyzing the potential impacts of large scale integration of electric vehicles into the power grid, the benefits and potential adverse effects are mainly discussed in Chapter 1. The methods for modeling the charging behaviors of EVs and the existing smart charging algorithms are introduced in Chapter 2, then two different smart charging algorithms are used in this research to coordinate the stochastic charging behaviors of EVs. The potential effects of large scale integration of EVs on power system reliability are analyzed in Chapter 3 and 4. The potential application of aggregated EVs providing operating reserve is also discussed in Chapter 4. The conclusion and future work are in Chapter 5.

Chapter 2

Smart charging control of EVs

2.1 Literature review of smart charging algorithms

The power and capacity level of a single EV is small, in order to achieve the economic and technical advantages in the energy and ancillary services bidding market, a unique market entity is needed to coordinate the charging behaviors of large amount of EVs. The role of aggregator [5, 32, 33] is introduced by some literatures, it contracts a significant number of EVs and works as an interface between the end users and energy market. The capacity of aggregator is determined by the controlled number of EV and the flexibility of each car, which depends on users' behaviors and preferences. With the aggregator, the smart charging can be implemented in two different control architectures, centralized and decentralized control methods. The functions and roles of aggregator will be variant under different architectures.

2.1.1 Centralized charging control

For the centralized control architecture, aggregator can directly control the charging behaviors of each cars. By collecting the historical data and users' preferences, the aggregator can predict its daily energy need and controllable capacity.

The forecast of energy need will be evaluated by the distribution system operator for system security. The time scale may be variant under different markets and operation situations, usually the aggregator will bid into the day-ahead electricity market for its energy need. The transmission system operator will also evaluate the potential effects on the transmission system. If all security based criteria are met and biddings cleared, the aggregator can achieve the charging control objective and provide the needed ancillary service by providing real time charging set points for each controlled EV, the whole process is shown in Fig. 2.1. The aggregator will also monitor the real-time operation of connected EVs and collect related information, like the identification, state of charge (SOC) and user preference settings. A wide range of algorithms with different objectives have been discussed in literatures.

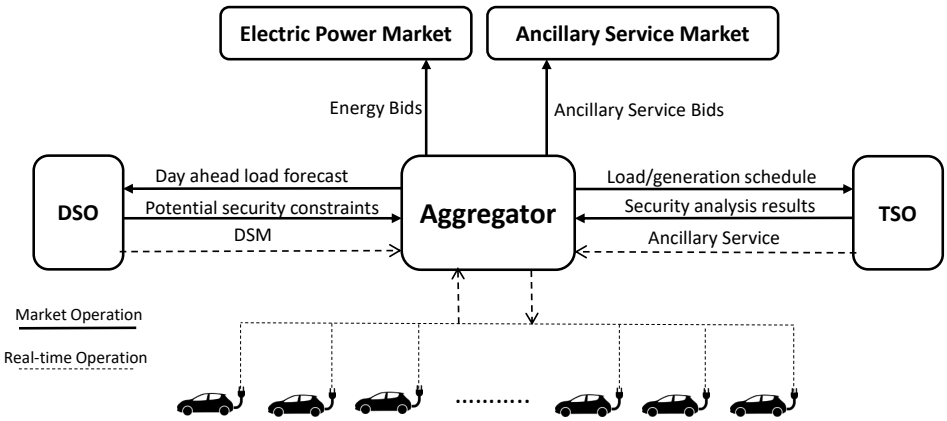

Figure 2.1: Centralized control architecture.

Coordinated charging

Han et al. [5] proposed an aggregator based market mechanism, which use the distributed electric vehicles to provide frequency regulation services to the grid by determining the charge schedule of each EV. The author pointed out when a vehicle battery is charged, it plays a role as the load to the grid which directly affect the frequency regulation control process if under a high EV penetration scenario. If the

load suddenly disappear (or adjusted) when the frequency regulation control is trying to achieve the delicate balance between power generation and load, it would affect the control loop. Aggregator will decides the charging rate, charging sequence, and duration to maximize the revenue, a dynamic-programming method is used to find the optimal charge schedule. Sortomme and El-Sharkawi [34] presented a similar charge control algorithm, which could take part into the frequency regulation by changing the charging set points. The aggregator controls the charging behaviors of each EV according to its capacity, the regulation up or down are achieved by simulating the decrease or increase of load. Wu et al. [35] put forward a centralized control framework. A minimum-cost load scheduling algorithm is designed to determine the amount of energy purchased in the day-ahead market, which is based on the forecast electricity price and EV power demands. Then a dynamic dispatch algorithm is developed to distribute the purchased energy to different EVs on the operating day. The impacts of aggregated EV load on the distribution grid is also studied.

V2G enabled smart charging

The literatures in last section focus on the control of charging schedule and charge rate, so the power flow is still unidirectional. Power flow is possible in both directions with the V2G technology. EV can provide more flexibility, but simultaneous charging and discharging of an EV battery is not allowed. Meantime, the battery degradation caused by discharging should be carefully evaluated.

Tan and Wang [36, 37] put forward a two-layer evolution strategy particle swarm optimization (ESPSO) algorithm to integrate PHEVs into a residential distribution grid, which is based on a stochastic model of PHEV. A novel business model is developed for PHEVs to provide ancillary service and participate in peak load shaving. The virtual time-of-use rate is used to influence the charging behaviors. The objective function includes the peak load shaving, power quality improvement, charg-

ing cost, battery degradation cost and frequency regulation earnings. Sortomme and El-Sharkawi [38] developed a V2G algorithm to optimize the energy and ancillary services scheduling. This algorithm maximizes the profits of aggregator by providing additional system flexibility and peak load shaving to the utility and low prices for EV charging. A hypothetical group of 10 000 commuter EVs in the ERCOT system were simulated, the results showed significant benefits for customers and aggregator. Khodayar et al. [39] coordinated the integration of aggregated plug-in electric vehicle (PEV) with renewable energy (wind energy) in power systems by stochastic security-constrained unit commitment (SCUC) model. The objective is to minimize the expected grid operation cost with the random behavior of PEVs considered. Customers' random behaviors of driving patterns, locational energy requirements, topological grid interconnections, and other constraints imposed by consumers are considered. The numerical case showed PEVs can help reduce the grid operation cost by providing energy storage for renewable energy resources. Jin et al. [40] studied the coordination of EV charging scheduling problem with Energy Storage (ES) from an electricity market perspective, with joint consideration of aggregator's energy trading in the day-ahead and real-time markets. The author pointed ES can be utilized by aggregator to mitigate the impacts of uncertainty and inaccurate prediction. A Mixed Integer Linear Programming (MILP) model as well as a simple polynomial-time heuristic based LP rounding are proposed to get optimal solutions. Tan and Wang [41, 42] proposed a hierarchical framework for plug-in hybrid electric vehicles to participate in frequency regulation in a deregulated market. At the upper level of the game, the competition between aggregators are formulated as a non-cooperative game. Markov game is then used to coordinate the charging behaviors of PHEVs at the lower level. The Markov game will optimize the regulation capacity bidding in the upper level game.

2.1.2 Decentralized charging control

Decentralized control is also known as indirect control, each EV has some level of intelligence and communication abilities to make charging decisions to achieve its own maximum benefits. Meantime, the aggregator can use price signal to influence the charging and discharging behaviors of EV. The system architecture is shown in Figure 2.2.

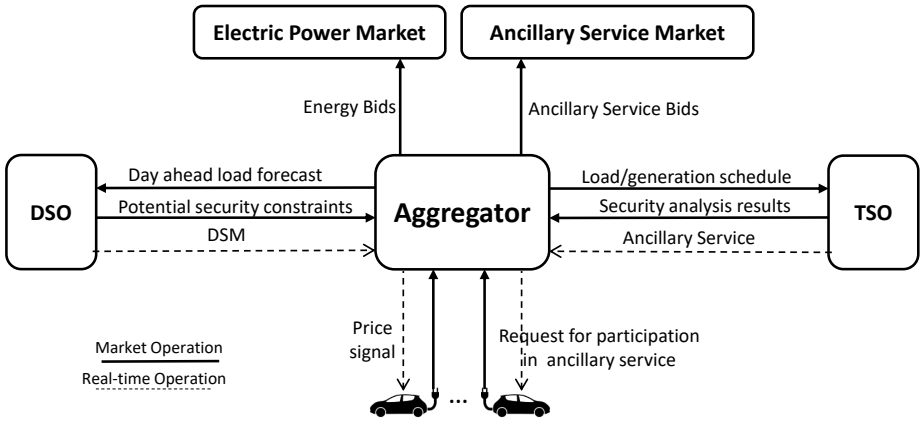

Figure 2.2: Decentralized control architecture.

Coordinated charging

Ma et al. [43] proposed a decentralized charge scheduling algorithm for a large number of EVs using the mean field game. The social optimality was achieved by establishing a PEV charging schedule that transfer the charging load to the night demand valley. The aggregator broadcasts the prediction of base demand to all EV agents, then each EV makes its own charging schedule decision that minimize its cost. In the third step, each EV modify its charging plan according to the new aggregated charging demand. Steps 2 and 3 are repeated until each EV has no incentives to change its strategy. The implementation issues and computational complexity were also discussed. Gan et al. [44] proposed a similar decentralized charge scheduling algorithm for EVs to fill the electricity valley demand. The objective is to minimize the

charge cost of the EVs within the targeted charging deadline. This work is different with [43], EVs updating their charging profiles according to the control signal, which is used by the utility company to influence the charging behaviors. This algorithm only requires each EV solve its own optimization problem, which has the benefit of low computation capability requirements. Wen et al. [45] used a charging selection concept for EVs to maximize user convenience levels while satisfying demand constraints. The convex relaxation optimization tool was used to reduce the complexity of the problem and to get the close-to-optimal solutions. A distributed optimization algorithm is also proposed in this research to solve the charging selection problem, which only needs each vehicle's power demand rather than private user state information, so this method can mitigate the increasing security and privacy concerns.

The idea of multi-agent system is also introduced in the EV smart charging control [47, 48, 49]. Karfopoulos and Hatziargyriou [48] proposed a distributed, multi-agent based EV charging control algorithm, which bases on Nash Certainty Equivalence Principle. Convergence of this method is discussed when EVs' control agents are in both uncoupled and weakly-coupled methods. The MAS system is developed in the Java Agent Development Framework (JADE). Logenthiran and Srinivasan [49] used the method of decentralized Multi-Agent System (MAS), a hybrid algorithm which combines Evolutionary Algorithm (EA) and a Linear Programming (LP) was used to manage the power distribution system with PHEVs. Simulation results showed the MAS approach is a scalable and robust decentralized methodology which can adapt incomplete and unpredictable information.

V2G enabled smart charging

The interactions among EVs and aggregators in the market for frequency regulation are studied by Wu et al. [50] using a new game-theoretic model. A pricing policy is used to encourage EVs to participate in frequency regulation, then a decentralized

control mechanism is proposed to guarantee the achievement of Nash Equilibrium in interactions between vehicles and aggregator. Fan [51] proposed a distributed framework for demand response and user adaptation in smart grid. The concept of congestion pricing in Internet traffic control was borrowed and the pricing information was proved to be useful to regulate the user demand. Ota et al. [52] proposed an autonomous distributed V2G control scheme, which could provide spinning reserve according to the frequency deviation. He et al. [53] proposed a global optimal scheduling scheme and a local optimal scheduling scheme for EV charging and discharging. In the global scheduling optimization, the charging powers are optimized to minimize the total cost of all EVs. Although the global optimal solution can achieve global minimal total cost, its impractical because the uncertain and stochastic information like the arrival time, charging periods of EVs are needed. So the author formulated a local scheduling optimization problem, which aims to minimize the total cost of the EVs. The outcomes showed the local optimal scheduling scheme can achieve a close performance compared with the global one.

2.2 The driving and energy characteristics of EVs

2.2.1 Driving pattern of EVs

The charging behaviors of EVs are greatly determined by the driving patterns, which will determine when, where and how much energy needed for charging. A typical driving pattern often starts at leaving home for work in the morning, having lunches at noon, backing to home at afternoon or maybe a short trip to the supermarket. Although the destinations and trips are very different for each car, the average daily mileage can be determined according to the probabilistic survey method [54], which is roughly 26 Miles.

Another important dataset for the simulation of driving patterns is National Household Travel Survey (NHTS) 2009 [55], which provides comprehensive information about the travel and transportation patterns in the United States. Data is collected from daily trips, which is taken in a 24-hour period and includes some important aspects like travel time, time of day when the trip took place, trip lengths, etc.

For the simulation of EV driving patterns, the time in a day when the trip takes place is defined as the departure time, the time in a day when EV arrives home is defined as the arrival time and the total drive distance in a day is defined as mileage. So according to the statistical data, the percentage of vehicles during different periods is shown in Figure 2.3, the similar one about the percentage of arrival time is shown in Figure 2.4.

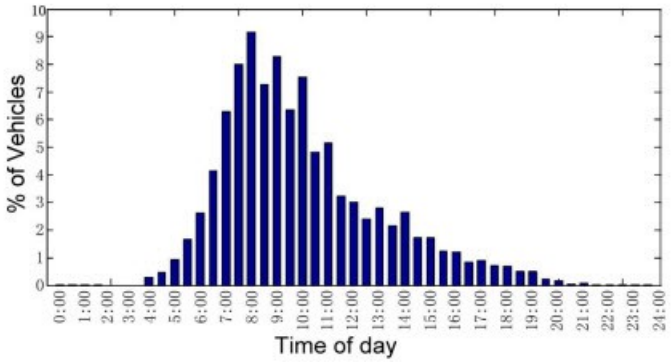

Figure 2.3: Percentage of vehicles versus departure time.

It is assumed the driving patterns of large amount of EVs will follow the statistical pattern, therefore the probability distribution functions of arrival time, departure time and mileage can be get from the survey data. As the figure of departure time shows, it follows the normal distribution:

$$F_d(t) = \frac{e^{-(t-\mu)/2\sigma^2}}{\sigma\sqrt{2\pi}},\ 0 < t < 24 \tag{2.1}$$

where μ=9.97, σ=2.2

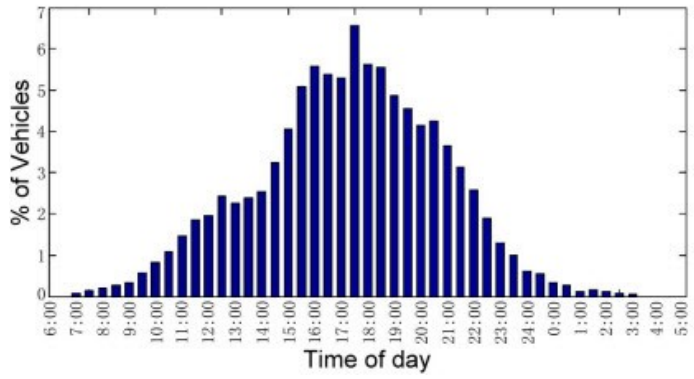

Figure 2.4: Percentage of vehicles versus arrival time.

Similarly, the probability distribution function of arrival time is expressed as:

$$F_a(t) = \frac{e^{-(t-\mu)/2\sigma^2}}{\sigma\sqrt{2\pi}},\ 0 < t < 24 \tag{2.2}$$

where μ=17.01, σ=3.2

The distribution of daily mileage can be described by a lognormal distribution function, which is shown in Figure 2.5, which is expressed as follows:

$$F_m(d) = \frac{e^{-(\ln d-\mu)/2\sigma^2}}{\sigma d\sqrt{2\pi}} \tag{2.3}$$

where d is the travel distance, unit is mileage. μ=3.2 is the mean value of $\ln d$ and σ=0.9 is the standard deviation value of this lognormal distribution function.

2.2.2 Charging characteristic of EVs

According to the charging capacity and charging methods, there are generally three kinds of charging methods [56]:

Level 1 slow charging is the most common method for electric vehicles charging. Level 1 charging usually use 120 V, AC plug, which can be standard household outlet. A full charge typically taking 8 to 12 hours, overnight charging at home is the most common type of charging cycle. Nearly all electric vehicle can be slow charged with

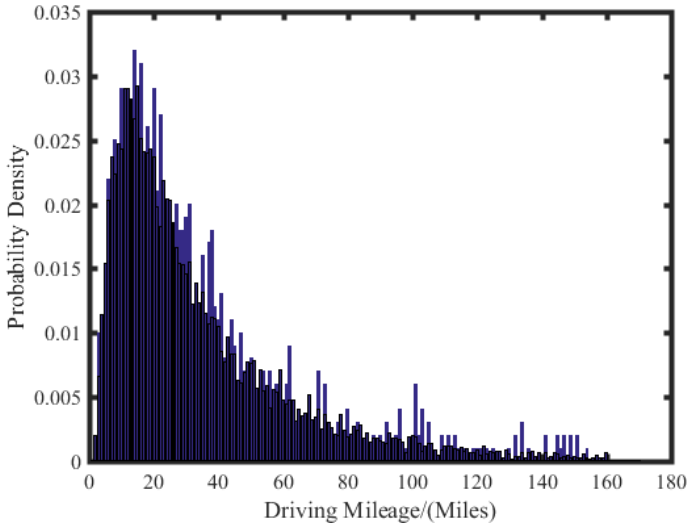

Figure 2.5: Daily driving mileage probability.

the appropriate connectors and cables. This kind of charging method has a relatively small charging power, so there is no need for EV owners to update the existing distribution feeder, however, with the increasing penetration rate, it may cost failures in the distribution network because of their variability and uncertainty.

Level 2 charging usually through a 240V, AC plug, which usually through installed home charging equipments or public charging stations. Level 2 charging is compatible with nearly all electric vehicles, the time for a full charge typically taking 4 to 6 hours.

Three are mainly two types of fast charging, rapid AC and DC charging. Rapid AC chargers provide a high power three phase AC supply. An electric vehicle can be charged to 80% in less than half an hour. Rapid DC chargers charges through a 480V, direct-current (DC) plug. The Tesla supercharger by consisting multiple chargers working together can deliver up to 120kW power. Both the rapid AC and DC charging methods are designed to meet the urgent charging need, which have very high power charging rate, so specific charging facilities and feeder lines are needed to guarantee its operation. The expensive of fast charging limit its application scale, so it mainly located at areas with high transportation rate.

2.2.3 The energy need of EVs' charging

Because of EV owner's mileage anxiety, it is reasonable to assume each EV owner will charge the battery to a full status before leaving for work next morning. And for the same reason, the minimum SOC is set to be 20%, which is also helpful for the battery lifetime. The all electric range (AER) of the electric vehicle is D_m. The electricity energy consumption of EV is proportional to the daily mileage, so the SOC of EV when arriving home is

$$SOC_{arrival} = \ (1 - D/D_m) \times 100\%, \quad 0 < D < 0.8D_m \tag{2.4}$$

The energy needed for charging after arriving home is:

$$E_r = \frac{1}{\eta} C_{EV} \cdot (1 - SOC_{arrival}) \tag{2.5}$$

where η is the energy efficiency of charging equipment, C_{EV} is the capacity of battery.

2.3 Distributed smart charging algorithm

2.3.1 Smart charging pricing mechanism

As analyzed before, one of the big problems of large scale EVs integration is the increased peak load, which may exceeds the existing generating capacity. Meantime, the increased peak load may also cause some detrimental effects on the transformer in the distribution system [20].

Smart charging control and time-of-use (TOU) tariff plan can significantly reduce the peak demand, so the optimization of the charging behaviors of EV is based on given variations in electricity prices, user preference and driving patterns, which can also avoid the extra generation capacity expansion [18]. A real time dynamic

Table 2.1: Charging characteristics of representatives EVs [57].

	Toyota Prius PHEV	**Chevrolet Volt PHEV**	**Nissan Leaf BEV**	**Tesla Roadster BEV**
Battery Capacity	4.4 kWh	16 kWh	24 kWh	53 kWh
All-electric Range	14 Miles	40 Miles	100 Miles	245 Miles
Connector Type	SAE J1772	SAE J1772	SAE J1772 JARI/TEPCO	SAE J1772
Level 1 Charging Rate	1.4 kW	0.96-1.4 kW	1.8 kW	1.8 kW
Charging Time	3 hours	5-8 hours	12-16 hours	30+ hours
Level 2 Charging Rate	3.8 kW	3.8 kW	3.3 kW	9.6-16.8 kW
Charging Time	2.5 hours	2-3 hours	6-8 hours	4-12 hours
Level 3 DC Fast Charging Rate	N/A	N/A	50+kW	N/A
Charging Time	N/A	N/A	15-30 minutes	N/A

pricing mechanism [37] is used in this research to reduce the peak load of the system, the charging price is changed with the system load, their relation is defined as:

$$\lambda(t) = \beta_1 + \beta_2 \cdot \alpha^{\frac{P_d^t - P_a}{P_a}} \tag{2.6}$$

where P_d^t is the system load demand (including EV charging load) at time t, P_a is the average load demand and β_1, β_2, α are price parameters, which are set as 0.1, 0.2 and 10 in this research. This smart charging price policy is sensitive to the load demand, when the system load increase, the charging price will also increase, especially during the peak load period.

2.3.2 Sequential charging price update mechanism

Each EV is an independent agent, which has the communication ability and intelligence to make decisions according to the existing information. When the EV agent is connected with the grid, it firstly enter into a planning queue. The relative positions of different agents in the queue are based on their connection time, which follows the policy of first come, first served. The EV agent on the top of planning queue receives the pricing signal from the aggregator agent, solves its own charging scheduling problem, report its charging schedule to the aggregator agent and then leaves the planning queue. The aggregator agent will keep updating the charging price information based on each EV agent's charging schedule and the system load.

Using this sequential charging price update mechanism, the charging prices only need to be updated for a single EV agent on the top of the planning queue, and the effect is only transmitted to the next EV agent in the queue. The communication requirements and computation complexity can be greatly reduced in contrast with the centralized control method, which needs updating control signals simultaneously for all EVs.

With the increasing integration ratio of renewable energy into the power system, the stochastic and intermittent nature of renewable energy will bring a lot of challenges on the system planning and safety, the stochastic nature of uncontrolled charging may make things worse. However, at the same time, the flexibility of EV can also be resources and solutions for the intermittency.

The distribution system operator (DSO) will monitor the system base load, EV charging and renewable energy generation, the potential violations of technical constraints, and contingencies. If technical constraints are violated, the DSO will require the aggregators in the control area to respond accordingly, for example, cut the charging load of aggregated EVs at current time step. The aggregator will then send an emergency signal to all connected EVs, the EV agent will enter into a reschedule

queue, similar with the planning queue. Each EV agent will solves its own charging scheduling problem for the remaining period before the departure based on its own energy needs and charging price information. Once solved, EV agent will leave the reschedule queue. The aggregator will update the charging price according to the updated charging schedules and required amount of charging load curtailments. The whole system architecture is shown in Figure 2.6.

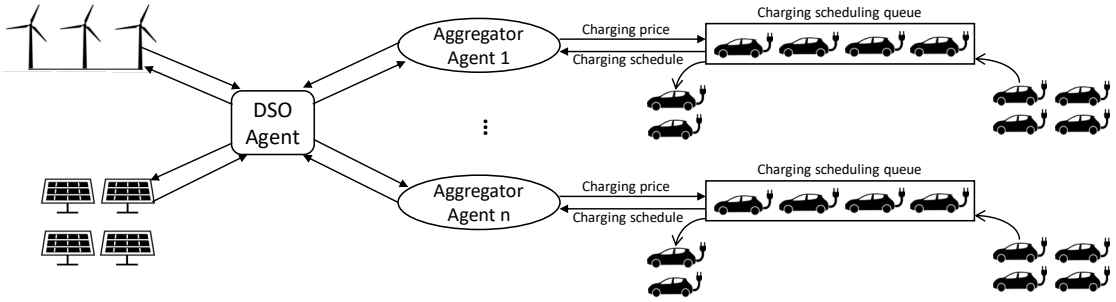

Figure 2.6: A multi-agent based distributed smart charging control architecture.

2.3.3 Problem formulation

The time horizon of EV charging is determined by the EV's arrival time and departure time. For the i_{th} EV, the time it arrives home is assumed to be the plug-in time $t_{i,in}$, which doesn't means the start of charging. The departure time of EV is assumed to be the time when the connector is plugged out, so the plug-out time is $t_{i,out}$. The energy need $E_{r,i}$ can be derived from Equation 2.5.

The behaviors of EV are controlled at two different status: charging and idle. The control sequence for EV i during the connected period can be expressed as:

$$K_i = \left[K_i^{t_{in}}, \cdots K_i^t \cdots K_i^{t_{out}}\right] \tag{2.7}$$

where K_i^t=1 means the i_{th} EV is charging at time t, K_i^t=0 means the EV is in idle status, no energy exchange with the grid.

The total energy required of the i_{th} EV can be expressed as Equation 2.8, which is also the energy constraint that smart charging algorithm must meets.

$$E_{r,i} = \sum_{t=t_{in,i}}^{t_{out,i}} K_i \cdot P_i \tag{2.8}$$

where P_i is the charging rate of i_{th} EV.

The related cost of charging for a EV is:

$$Cost_C = \sum_{t=1}^{T} P_{EV,C}^{t} \cdot C\left(t\right) \cdot \lambda\left(t\right) \tag{2.9}$$

where $\lambda\left(t\right)$ is the charging price for i_{th} EV, which comes from the combination of smart charging pricing mechanism and sequential charging price update mechanism.

The objective of each EV is to minimize its own charging cost, the constraint is the total energy requirement. By combining two different pricing mechanisms, the aggregator can affect the charging behaviors of EV through price signal, which is closely related with the real time load. So the distributed smart charging control is achieved by the combination of each vehicle's charging optimization problem, the problem solving is discussed in next section.

2.3.4 Binary hybrid GSA-PSO optimization algorithm

As mentioned in last section, the optimization problem of each vehicle's charging schedule is the key for the distributed smart charging algorithm. The GSA-PSO hybrid optimization method is used for this problem, which combines the gravitational search algorithm (GSA) and particle swarm optimization (PSO). Because EV's charging scheduling is a discrete optimization problem, so the hybrid continuous GSA-PSO algorithm is modified into a binary optimization method.

The hybrid method PSOGSA was first proposed in 2010 [58], the performance has been proved in the optimization problems solving. The search for optimization is

still done by the agents in the PSO, which is modified to mimic the agents' behavior in the GSA. So this hybrid method can use both the social thinking of PSO and the exploitation ability of GSA. The social thinking of PSO can alleviate the slow exploitation rate, which is the main drawback of the GSA.

Each search agent has a position vector, which reflects the agent's current position in search spaces:

$$X_i = \left(x_i^1, \cdots, x_i^d\right), \ i = 1, 2, 3, \cdots, N \tag{2.10}$$

where d is the dimension of the problem, x_i^d is the position of the i_{th} agent in the d_{th} search dimension, N is the number of search agents.

The idea of gravitational force are borrowed form GSA, firstly the euclidian distance and the gravitational constant between two search agents are defined as:

$$D_{ij}(t) = \sqrt{\left[x_i^1(t) - x_j^1(t)\right]^2 + \left[x_i^2(t) - x_j^2(t)\right]^2 + \cdots + \left[x_i^d(t) - x_j^d(t)\right]^2} \tag{2.11}$$

$$G(t) = G_0 \cdot exp\left(-\alpha \cdot citer/miter\right) \tag{2.12}$$

where G_0 is the initial gravitational constant, α is the descending coefficient and *citer* is the current iteration number, *miter* indicates the maximum iterations number.

The force between agent j on agent i at a specific time t can be defined as:

$$F_{i,j}^d(t) = G(t) \frac{M_{aj}(t) M_{pi}(t)}{D_{ij}(t) + \xi} \left[x_j^d(t) - x_i^d(t)\right] \tag{2.13}$$

where $G(t)$ is the gravitational constant value at t, $M_{aj}(t)$ is the active gravitational mass of agent i, $M_{pi}(t)$ is the passive gravitational mass of agent i, D_{ij} is the euclidian distance between agent i and agent j, ξ is a small constant number.

So for a search space with a dimension of d, the total forces on agent i at time t can be calculated as:

$$F_i^d(t) = \sum_{j=1}^{N} F_{i,j}^d(t) \cdot rand \ \ (j \neq i) \tag{2.14}$$

where $rand$ is a random number, which is generated by an uniform distribution in the interval of [0, 1].

With the total forces on an agent, the Newton's Second Law of Motion-Force and Acceleration is used to calculate the acceleration of agent i, which is proportional to the net force acting upon and inversely upon the mass of the object.

$$a_i^d(t) = F_i^d(t) / M_i(t) \tag{2.15}$$

where $M_i(t)$ is the inertial mass of agent i.

In the GSA, the weight of agent is calculated by the fitness function, which directly affect its movement. The agent with better fitness value will have bigger masses, then it will move slowly. For the GSA, during the process of agents moving towards the optimal point, the masses of agent will become heavier and heavier. In the final steps of iterations, the agents near the optimal point have almost same mass. According to the Newton's Second Law of Motion-Force and Acceleration, they gravitational forces between different agents are nearly same, which makes the movement speeds of agents very slow. However, combined with the PSO, the best solution so far is saved as $gbest$, which can guide the heavy agents move toward the optimal point, so the velocity update function which combines PSO and GSA is:

$$V_i(t+1) = V_i(t) \cdot rand + \beta_1 \cdot a_i^d(t) + \beta_2 \cdot [gbest - X_i(t)] \tag{2.16}$$

where $V_i(t)$ is the velocity of agent i, β_1 and β_2 are accelerating factors.

However, adding the *gbest* to the velocity vector will weaken the exploration in the early period of optimization, because it establishes a permanent element of velocity updating, so an adaptive method is used to change the accelerating factors β_1, β_2 adaptively during the iteration, the variations are shown in Figure 2.7.

$$\begin{aligned} \beta_1 &= -2(citer)^3/(miter)^3 + 2 \\ \beta_2 &= 2(citer)^3/(miter)^3 \end{aligned} \tag{2.17}$$

During the iteration process, the update function of agent's position is:

$$X_i(t+1) = X_i(t) + V_i(t+1) \tag{2.18}$$

So the whole procedures can be summarized as:

Step 1: Generate initial population, set the initial positions, velocities, masses and gravitational constant G_0.

Step 2: Calculate the fitness value for each agent.

Step 3: Update the G with Equation 2.12 and *gbest*.

Step 4: For each agent, calculate all gravitational forces using Equation 2.14, calculate the acceleration with Equation 2.15, update its velocity and location with Equation 2.16 and Equation 2.18.

Step 5: Repeat the Step 2-4 until satisfying the stop criterion

Step 6: Return the value of *gbest*.

In order to solve the binary optimization problem, the agent's position update function needs to be modified. A transfer function map the velocities to the probability for updating the positions, so the range of the function should be [0,1] and

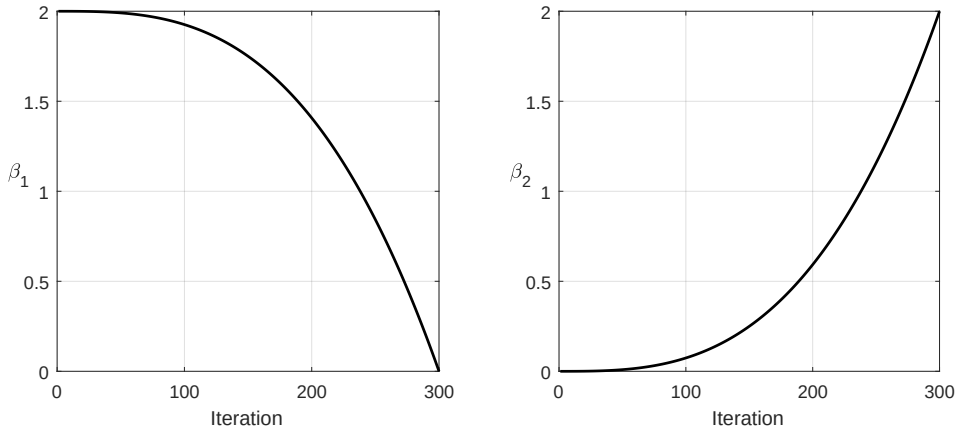

Figure 2.7: Adaptive parameters of accelerating factors.

increases with the velocity. The transfer function used in this research is $S[V_i(t)]$, which is shown in Figure 2.8.

$$S[V_i(t)] = |tanh(V_i(t))| \tag{2.19}$$

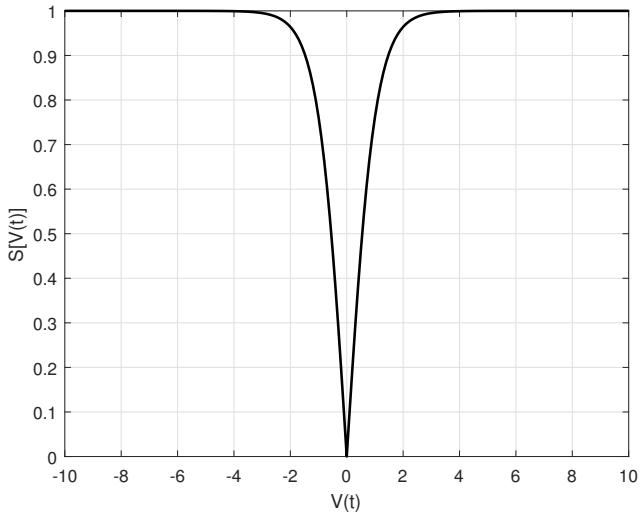

Figure 2.8: Transfer function for binary optimization.

The velocities of agents are transferred to the probabilities of position update, so the agent's position update function is:

$$\begin{aligned} &If\ S\left[V_i\left(t\right)\right] > rand, then\ X_i\left(t+1\right) = 1 - X_i\left(t\right) \\ &else\ X_i\left(t+1\right) = X_i\left(t\right) \end{aligned} \tag{2.20}$$

Compared with the GSA, the BPSOGSA has better exploitation ability because of the introduction of the social behaviors in PSO, which enables more accurate exploit around the best agent obtained so far. Meantime the intrinsic nature of GSA, where searching agents have impacts on each other during the whole iteration process is different with the PSO that only the local best and global best means.

At the same time, the adaptive parameters design of β_1 and β_2 making the algorithm has better exploration ability in the initial iterations. Then the exploitation ability increase during the iteration process to find the global optimal point. This mechanism can help the optimization searching process avoiding the local optimal points and accelerating the convergence speed towards the global optimal point.

2.4 V2G enabled smart charging algorithm

2.4.1 Problem formulation

The mathematical model is similar with the decentralized smart charging algorithm in last section. The time horizon of EV charging is determined by the EV's arrival time and departure time. For the i_{th} EV, the time it arrives home is assumed to be the plug-in time $t_{i,in}$, which doesn't means the start of charging, the departure time of EV is assumed to be the time when the connector is plugged out, so the plug-out time is $t_{i,out}$. The energy need $E_{r,i}$ can be get from Equation 2.5.

The behaviors of EV at this scenario are controlled at three different status: charging, discharging and idle, the control sequence for the i_{th} EV during the con-

nection period can be expressed as:

$$\boldsymbol{K_i} = \left[K_i^{t_{in}}, \cdots K_i^t \cdots K_i^{t_{out}}\right] \tag{2.21}$$

where K_i^t=1 means the i_{th} EV is charging at time t, $K_i^t = -1$ means the i_{th} EV is discharging at time t and K_i^t=0 means the EV is in idle status.

The total energy required of the i_{th} EV can be expressed as Equation 2.22, which is also the energy constraint that the smart charging algorithm must meets. P_i is the charging rate of i_{th} EV.

$$E_{r,i} = \sum_{t=t_{in,i}}^{t_{out,i}} \boldsymbol{K_i} \cdot P_i \tag{2.22}$$

The status vectors $\boldsymbol{C_i}$ and $\boldsymbol{D_i}$ are used to separately indicate the charging and discharging status of each vehicle, which are defined as:

$$\boldsymbol{C_i} = \left[C_i^{t_{in}}, \cdots C_i^t, \cdots C_i^{t_{out}}\right],\ C_i^t = \begin{cases} 1, & if\ k_i^t = 1 \\ 0, & otherwise \end{cases} \tag{2.23}$$

$$\boldsymbol{D_i} = \left[D_i^{t_{in}}, \cdots D_i^t, \cdots D_i^{t_{out}}\right],\ D_i^t = \begin{cases} 1, & if\ k_i^t = -1 \\ 0, & otherwise \end{cases} \tag{2.24}$$

The total charging power of n EVs is illustrated as:

$$P_{EV,C}^t = \sum_{i=1}^{n} \boldsymbol{C_i} \cdot P_i \tag{2.25}$$

The related cost of charging is:

$$Cost_C = \sum_{t=1}^{T} P_{EV,C}^t \cdot C\left(t\right) \cdot \lambda\left(t\right) \tag{2.26}$$

where $\lambda(t)$ is the real time charging price get from Equation 2.6, which is closely related with the system load.

The total discharging power of n EVs is illustrated as

$$P_{EV,D}^{t} = \sum_{i=1}^{\mathrm{n}} \boldsymbol{D_i} \cdot P_i \tag{2.27}$$

The total energy discharge during the whole time is

$$E_D = \sum_{i=1}^{n} \sum_{t=t_{i,in}}^{t_{i,out}} \boldsymbol{D_i} \cdot P_i \tag{2.28}$$

The related revenue of discharging is

$$Earn_D = \sum_{t=1}^{T} P_{EV,C}^{t} \cdot D(t) \tag{2.29}$$

When it comes to discharging, the problem of battery degradation needs to be carefully analyzed. Chenke et al. [59] built a mathematical model for the cost of EV battery degradation because of V2G. Combined with manufacturer's data, the results showed the DoD and ambient temperature are two most significant influence factors on the battery life. However, because of the ambient temperature is a stochastic variable, so a simplified model is used in this research, the cost of battery degradation [60] is expressed as:

$$Deg_D = \frac{c_b \cdot E_b + c_L}{L_c \cdot E_b \cdot DoD} E_D \tag{2.30}$$

where c_b is the unit capacity cost for battery, \$/kWh, E_b is the capacity of battery, c_L is the labor cost for the replacement of battery, L_c is the battery life cycle times at a predefined level of DoD, DoD is the depth of discharge, it refers to the an ratio between the absolute discharge and the rated battery capacity. It's hard to directly get the real operational data of DoD, so the $(1 - SOC)$ is used to represent the DoD of EV battery. E_D is the energy discharge because of V2G, which can be get from

Equation 2.28. In this research, the c_b, c_L are set as 300 \$/kWh and 240 \$, the L_c is set as 5000 at 80% discharge [61].

The objective function of this optimization problem is minimizing the total cost, which can be represented as:

$$min\,(Cost_C + Deg_D - Earn_D) \tag{2.31}$$

2.4.2 Intelligent PSO algorithm

For the centralized optimization architecture, the aggregator needs collect information about each EV, finds the optimization point and directly sends control signal to each vehicle. So if the aggregator controls a large number of EVs, like thousands, the search space for this optimization will be very large and falls into the curse of dimensionality. Meantime, the frequent status switching between charging and discharging will greatly reduce the life time of battery [61], so the control sequence should be wisely arranged.

Based on this presumption, the search space is simplified by using the dominant solution matrix. Based on different V2G strategies, the control sequences $\boldsymbol{K_i}$ are classified into different patterns. For a single EV, firstly it can choose a row from the dominant matrix [37], which stands for different V2G patterns, then the starting point of the row will determine the specific control sequence of the EV. The schematic diagram of dominant search matrix is shown in Figure 2.9.

So it's basically a two layers evolution PSO optimization algorithm, the optimal V2G strategy is firstly set on the upper level, then based on that strategy the optimal control sequence is find in the lower level. Each EV is a dimension in the search space, the sequence starting point is mapped as the variable number in that dimension, the evolving process is guided by the following equations:

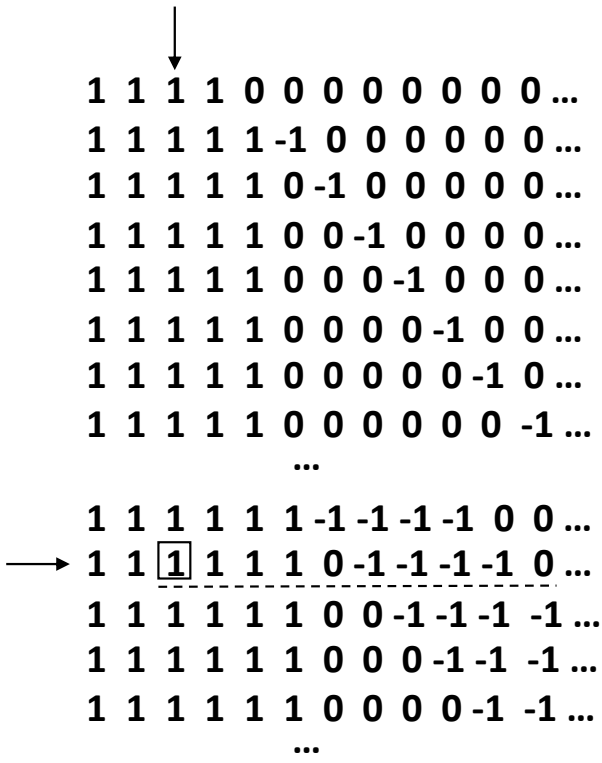

Figure 2.9: Schematic diagram of dominant search matrix.

$$KE_i^n = K_i^n + \omega N\left(0, \sigma_d\right) \tag{2.32}$$

$$K_i^{n+1} = \begin{cases} KE_i^n,\ if\ cost\left(KE_i^n\right) < pbest_n \\ K_i^n,\ otherwise \end{cases} \tag{2.33}$$

$$\omega = \omega_{max} - n\frac{\omega_{max} - \omega_{min}}{n_{max}} \tag{2.34}$$

$$V_i^{n+1} = \sigma V_i^n + \beta_1\ rand_1\left(pbest_i - X_i^n\right) + \beta_2\ rand_2\left(gbest - X_i^n\right) \tag{2.35}$$

$$X_i^{n+1} = X_i^n + V_i^n \tag{2.36}$$

where K_i^n is the original V2G strategy, the KE_i^n is the evolved one, ω is the inertia weight, n is the iteration number, i is the i_{th} particle agent. The velocity V_i^n and position X_i^n of agent are constantly updated during the evolving process.

2.5 Numerical study

As introduced before, the level 1 charging has a slow charge speed, usually take 8-12 hours for a full charge, Level 2 charging equipment is compatible with all electric vehicles and plug-in electric hybrid vehicles, the time for a full charge typically take 4 to 6 hours. As the battery capacity and energy density increases, the Level 2 charging will be more popular with customers. So in this research, it assumes all electric vehicles will return home for charging and use the Level 2 charging method, the charging rate is set as 3.3kW. In the V2G enabled smart charging algorithm, all charging equipments are considered to have the capabilities of discharging energy into the grid and metering, the discharging rate is set as the same as charging rate.

In order to show the effect of EVs' charging on system and the performance of proposed smart charging algorithms, a test system is designed for the numerical analysis, the load without EV charging in each hour is shown in Table 2.2.

Table 2.2: Base load of the test system without EVs charging (Unit:MW).

Hour	**1**	**2**	**3**	**4**	**5**	**6**	**7**	**8**
	3.2657	2.9668	2.7193	2.8169	2.9692	3.2292	3.5436	3.8767
Hour	**9**	**10**	**11**	**12**	**13**	**14**	**15**	**16**
	4.3895	4.7274	4.8928	4.9943	5.1120	5.0652	5.1657	5.3538
Hour	**17**	**18**	**19**	**20**	**21**	**22**	**23**	**24**
	6.1084	6.6810	7.3053	7.2772	7.0025	6.2714	5.2944	4.2392

2.5.1 Distributed smart charging control

For the distributed charging control algorithm, each EV agent has some level of intelligence to make decisions about its own charging schedule with the known system information, so the complexity and computation burden of this optimization problem must be well handled. So for this problem, after several experiments, the number of agents in the binary hybrid GSA-PSO optimization method is set as 60.

The convergence curve of agents in this algorithm is shown in Figure 2.10, the fitness value of agent is the charging cost of each EV agent. As the figure shows, all agents can converge to the optimal point very rapidly after 20 iterations, so in order to improve the computation efficiency, the maximum iteration number is set as 40.

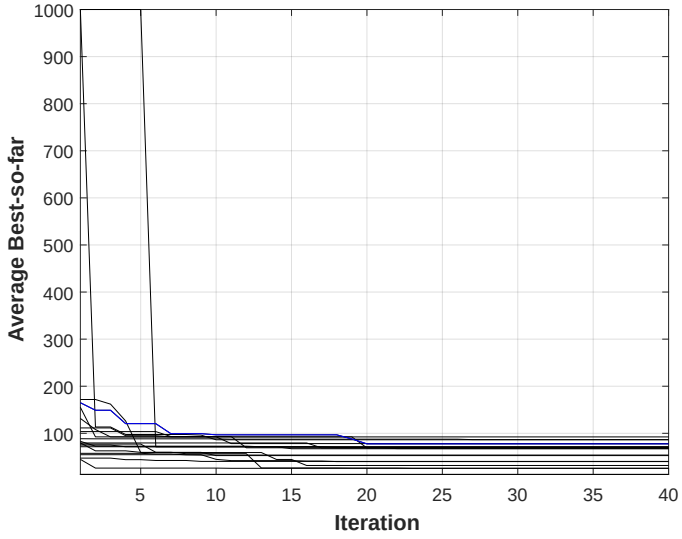

Figure 2.10: The convergence curves of 20 agents in the BPSOGSA.

With the same charging control algorithm, the integration ratio of electric vehicles will have a determining effect on the system load. When the EV number is relatively small, like 100 in Figure 2.11, the uncontrolled charging method will slightly increase the system peak load and the effect of smart charging is not so evident. So under a low integration rate, the existing distribution network doesn't need upgrade.

However, when the number of EV increased to 1000 as the Figure 2.12 shows, the uncontrolled charging under this scenario can increase the system peak load to nearly 11MW at 9 pm. The purpose of this smart charging algorithm is flattening the load curve, so the peak load nearly keep the same, the existing charging needs are transferred to the night valley hours. Compared with the system base load, we can find the charging load start to increase after 10 pm and mainly concentrate on the

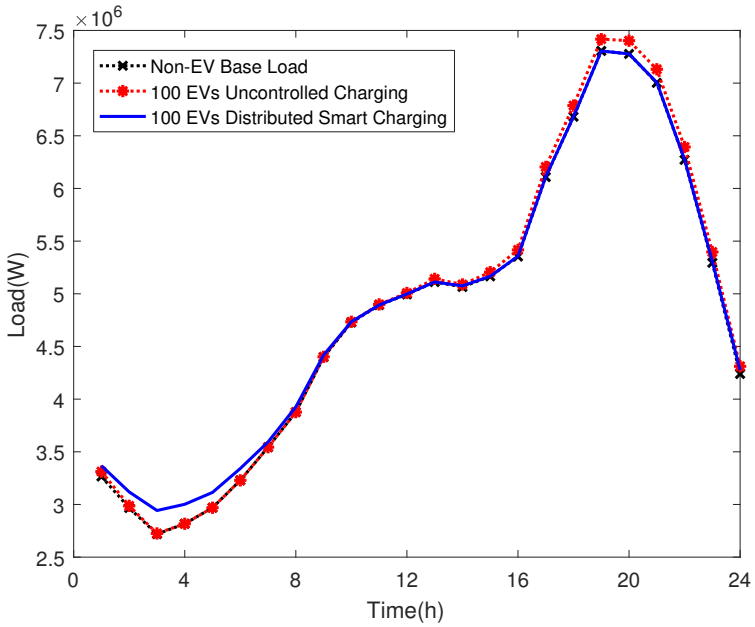

Figure 2.11: System load with 100 EVs under different charging control algorithms.

night valley hours. The effect of flattening the load is more evident with the scenario of 3000 EVs in Figure 2.13.

In order to show the performance of smart charging algorithm on flattening the load curve in a quantitative way, a comparison between the peak and valley load value with different charging algorithms is shown in Table 2.3. The results show the smart charging algorithm can effectively reduce the peak-valley load difference and flatten the load curve.

Table 2.3: Comparison of peak and valley load with different EV charging algorithms.

	Base load	Uncontrolled Charging		Smart Charging	
		1000 EVs	3000 EVs	1000 EVs	3000 EVs
Peak load P_p	7.3053	8.4768	10.8735	7.3119	7.3218
valley load P_v	2.7193	2.8404	3.0125	4.4372	5.5188
Peak and valley difference P_d	4.5860	5.6364	7.8610	2.8747	1.8030
P_d/P_p %	62.78	66.49	72.30	39.32	24.63
P_d/P_v %	168.65	198.44	260.95	64.79	32.67

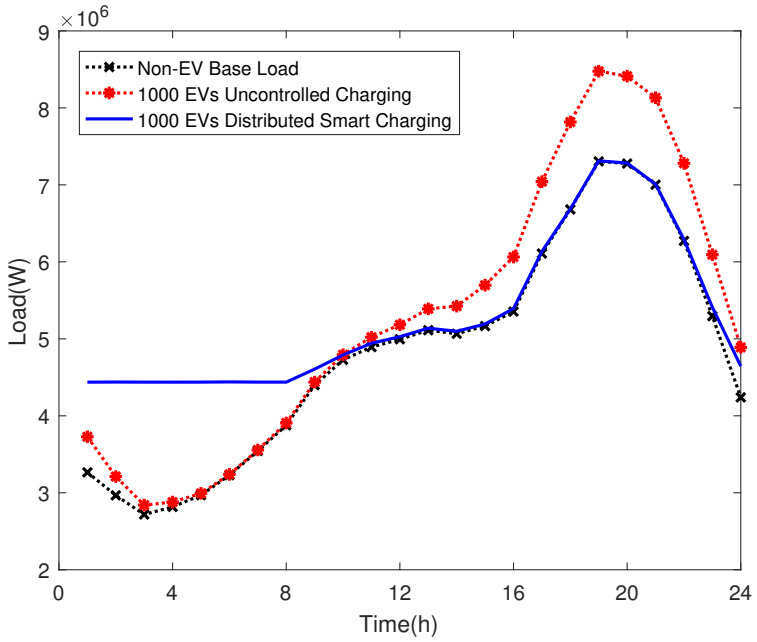

Figure 2.12: System load with 1000 EVs under different charging control algorithms.

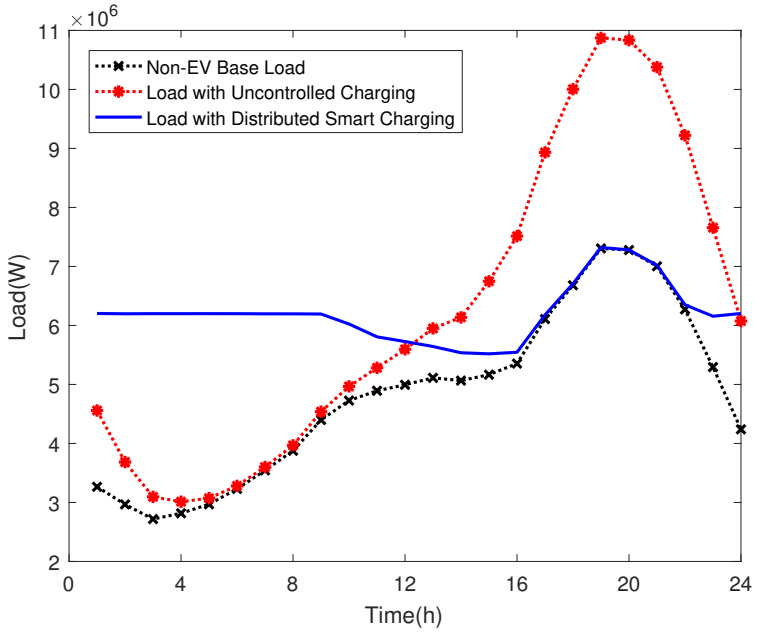

Figure 2.13: System load with 3000 EVs under different charging control algorithms.

2.5.2 V2G enabled smart charging control

For the V2G enabled smart charging, the same test system in Table 2.2 is used, the results in last section show the difference under different EV integration ratio, so this case only focus on the 3000 EVs scenario. With the V2G enabled smart charging control, electric vehicles could discharging energy into the grid to earn the revenue, if the related revenues large enough. The optimization objective of the centralized aggregator is to minimize the total cost in Equation 2.31, which is the cost of charging and battery degradation minus the revenues from V2G discharging. The system load with this V2G enabled smart charging is shown in Figure 2.14.

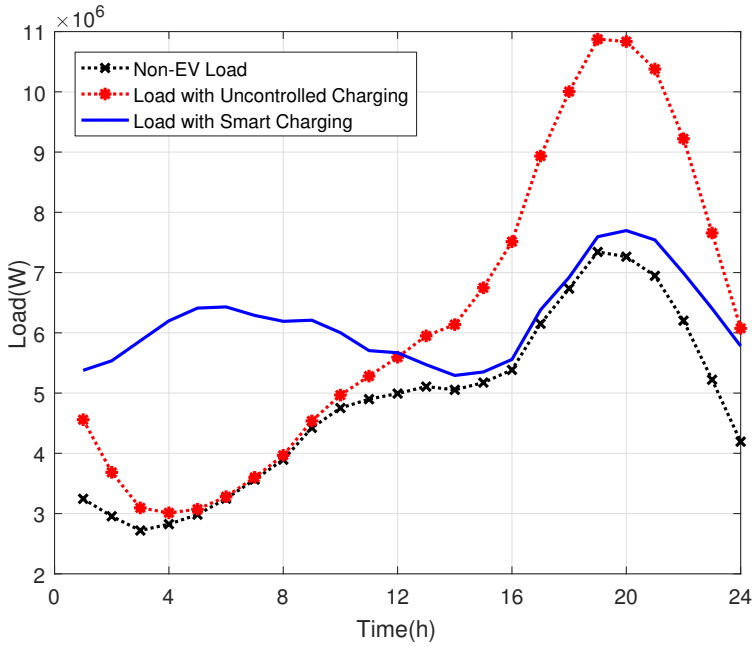

Figure 2.14: System load with 3000 EVs under different charging control algorithms.

The results shows this algorithm can also flatten the load curve very well, especially it can reduce the system load peak at 9 pm a lot. Because the smart pricing mechanism is also used in this algorithm, this charging pricing mechanism is very sensitive to the load variation, especially during the peak load hour. If there is no smart charging control, the increased peak load caused by uncontrolled EV charging can cause a very high price for EV charging, which is shown in Figure 2.15. However,

with the smart charging, the charging load is transfered from the peak load hour to the night hour, so the charging price at the peak hour also decrease a lot.

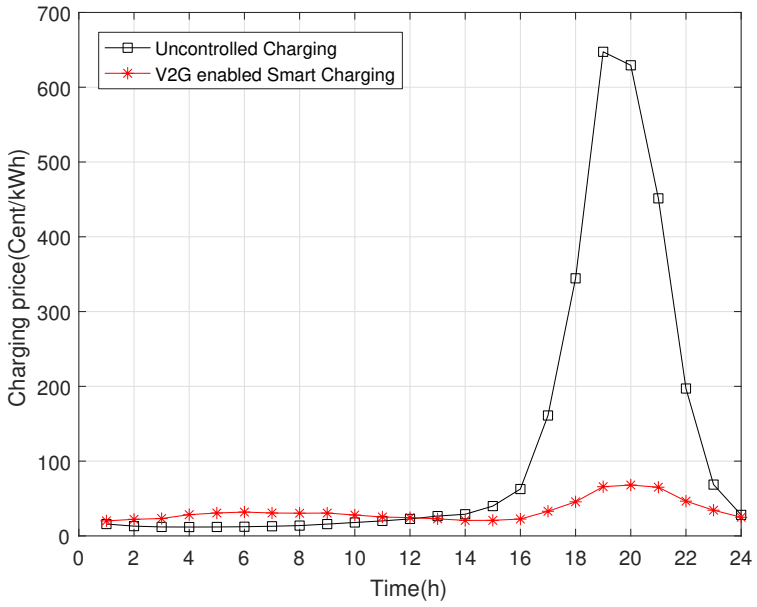

Figure 2.15: The charging price for different charging control algorithms.

As mentioned before, the EV can discharging energy into the grid with V2G technology, so for the specific load model, the net charging power of aggregated 3000 EVs is shown in Figure 2.16. The results show the charging loads are mainly concentrate on the night valley load period, and the net charging load of aggregated EV during the peak load hours is minus, which means the aggregated EV at this period is playing the role of distributed generation. With more attractive discharging price, the amount of discharging power can be much larger. And there are many potential applications with aggregated and V2G enabled EVs, such as frequency regulation, providing operating reserve. The application of providing operating reserve for the power system and its effects on reliability will be discussed in Chapter 4.

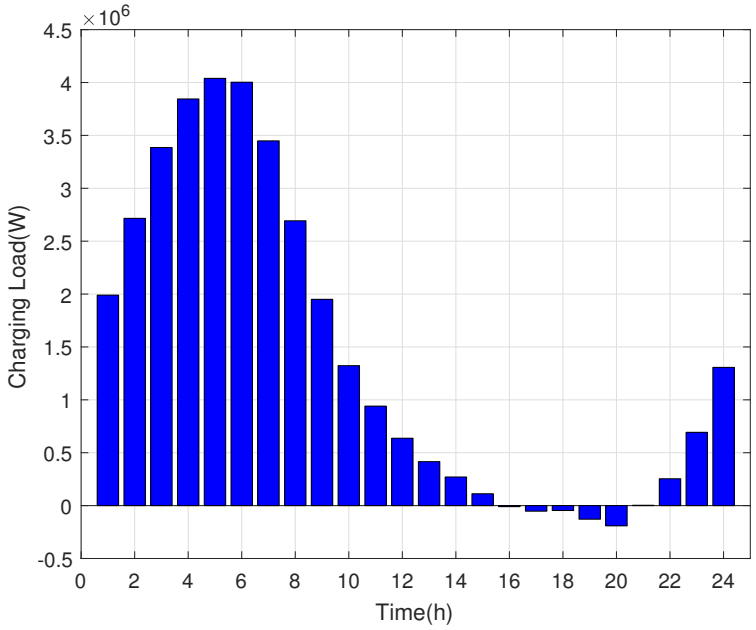

Figure 2.16: Net charging load of aggregated 3000 EVs.

Chapter 3

The effects of large scale integration of EVs into the grid on power system reliability

3.1 Power system reliability analysis introduction

The power system is the largest man-made system that ever existed on the earth, it's so complex and delicate that requires the electric power is produced by the generating units and transmitted to the end users through transmission system in real time, because there is no economic and convenient method for electric power storage.

The power system reliability is often defined as the probability of power system could deliver electric power to the end user on a continuous period with acceptable service quality [62]. According to the characteristics of power system, the reliability analysis is based on hierarchical levels, all three major parts of power system are included and combined into different hierarchical levels, as the Figure 3.1 shows. The hierarchical level 1 analysis only including the generating system, hierarchical level

2 includes both the generating and transmission system, which is often called the composite system or bulk power system, and hierarchical level 3 includes all three major parts of power system. However, the hierarchical level 3 analysis is not usually done because of its complexity.

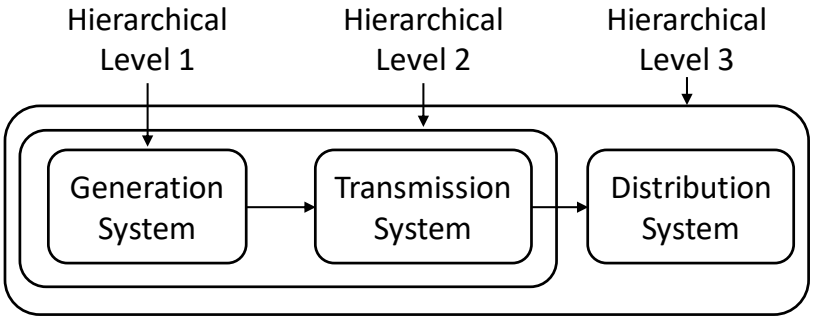

Figure 3.1: Hierarchical levels of power system reliability assessment [63].

The reliability evaluation plays important roles in both the planning and operating process. Long term reliability analysis is usually used in the relatively long term system planning, for example, determining whether the system has sufficient generating capacity to meet the load demand, determining whether the transmission system has sufficient capacity to transfer the energy to the customers on end points. However, for the power system operating, the uncertainty and contingencies will endanger the safe and reliable operation of the power system and then affect the customers, so the short term power system reliability which could assist the system operator is needed, such as determining the capacity of operating reserve. This chapter will discuss the effects of smart charging on the long term power system reliability.

3.1.1 Methods of reliability evaluation

The power system has used the deterministic methods for the planning and operation for decades. However, the system nature is stochastic, this characteristics is more evident in recent years with an increasing integration ratio of intermittent

renewable energy and electric vehicles, which brings a lot of challenges on the safe and reliable operation of power system. So more and more utilities have switched to the statistical and probabilistic methods [64]. With valid data collected by the utilities, such as the system availability, the number of hours of interruption, the probabilistic methods can offer a more precise model of the stochastic system, then help the unities achieve the delicate balance between the reliability and cost, as the Figure 3.2 shows.

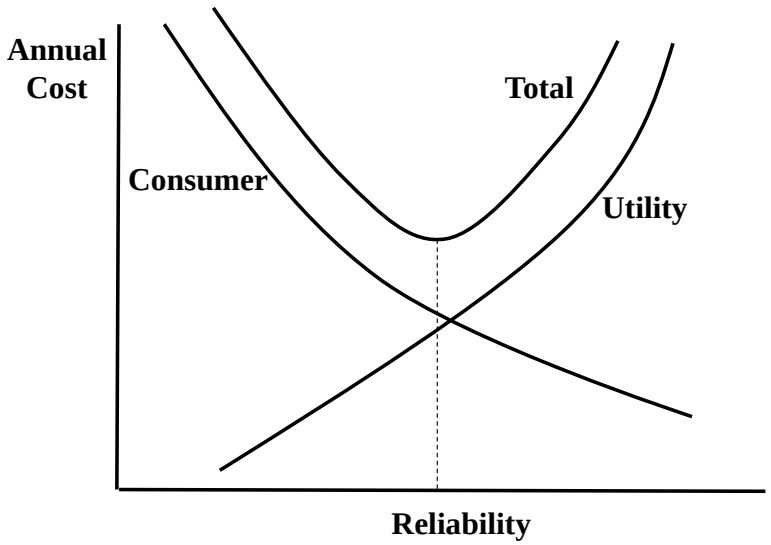

Figure 3.2: Total reliability cost of the system [63].

There are basically two probabilistic methods: analytical and simulation method. The traditional method is the analytical one, which could provide sufficient information to the system planners and operator. However, with the rapid development in computation ability, the simulation method especially the Monte Carlo Simulation (MCS) has gained a lot of interest in recent years [65, 66].

The analytic methods use the mathematical model of the system and get the reliability indexes using the direct numerical solutions, it can get the indexes in a short time. However because of the complexity of the real system, the analytic method has to make assumptions to simplify the problem and produce a solvable

mathematical model, this model maybe loss some or much significance when dealing complex systems or complex system operations, so the simulation methods are needed. The simulation methods take a different path to estimate the reliability indexes by simulating the system operation, the random events like the unit failures and outages are considered as different simulation cases, therefore the simulation methods have the ability tp model all the contingencies in the power system. The states of units in the simulation process are randomly generated according to the statistical indexes, the combination of units' status comes to the system status. The status occurred with high frequency means high probability in the real world. So a high number of simulations are needed for an accurate estimation of reliability indexes, which would cost a huge computation burden and is the main drawback of simulation methods.

According to the sampling methods, the Monte Carlo Simulation methods can be divided into two categories: non-sequential and sequential. For the non-sequential sampling, the system state is obtained by combining the sampled status of all components. The sequential method sampling the stochastic status of components in a sequential method, which is suit for the chronological representation of the system, the details about how this method is used in power system reliability evaluation will be discussed in later section.

3.1.2 Generating system reliability analysis

The most important index for the generator in the generating reliability analysis is its operation status. If a two state model is used to represent the unit status, like the Figure 3.3, the probability of a unit on outage status is defined as the unavailability, also known as the unit forced outage rate (FOR). This parameter is often used for the reliability evaluation during a relatively long period, all status that unit is not working (such as maintenance) are included into the unavailable situations. If the analysis cycle is short, then the more accurate four state model is needed.

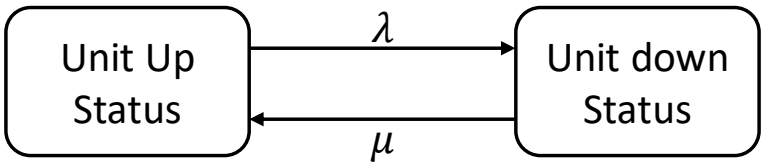

Figure 3.3: Two states model of generating unit

$$Unavailability = \frac{\lambda}{\lambda+\mu} = \frac{r}{m+r} = \frac{r}{T} = \frac{f}{\mu} = \frac{\sum[DownTime]}{\sum[DownTime]+\sum[UpTime]} \quad (3.1)$$

$$Availability = \frac{\mu}{\lambda+\mu} = \frac{m}{m+r} = \frac{m}{T} = \frac{f}{\lambda} = \frac{\sum[UpTime]}{\sum[DownTime]+\sum[UpTime]} \quad (3.2)$$

where λ is the expected failure rate, μ is the expected repair rate, m is the mean time to failure=$1/\lambda$ =MTTF, r is the mean time to repair=$1/\mu$=MTTR, f is the cycle frequency and T is the cycle time, $T = 1/f$.

3.1.3 Reliability indexes

With the generating system's model illustrated in last section and a proper load model, the system risk index can be calculated to show the reliability status of this system. With different load models, the risk indices are also different. One of the most simple model is using the daily peak load to represent the load in a day, once the capacity of generating system smaller than the system load level, a loss of load situation occurs. Combined with the capacity outage capacity table (COPT), the expected number of days in which loss of load happens during the reliability evaluation period can be get. The reliability index under this kind of scenario is loss of load expectation (LOLE). If a more detailed load model is available, the LOLE index can also be calculated based on the hourly load.

$$LOLE = \sum_{i=1}^{n} P_i \left(C_i - L_i\right) \quad (3.3)$$

where $P_i\,(C_i - L_i)$ is the possibility of loss of load (available capacity is exceeded by the load during the period i), which can be directly obtained from the cumulative probability in the COPT.

The LOLE shows the reliability status in the aspect of possibility, which doesn't give information about how much energy losses due to the loss of load, therefore the energy index of reliability like loss of energy expectation (LOEE) is used to show the expected energy curtailment due to the capacity outage scenarios.

$$LOEE = \sum_{i=1}^{n} P_i E_k \tag{3.4}$$

The LOEE can be normalized as:

$$LOEE_{p.u.} = \sum_{i=1}^{n} \frac{P_i E_k}{E} \tag{3.5}$$

The normalized LOEE stands for the ratio of curtailed energy due to the deficiencies in generating capacity and the total energy needed to meet the energy need of demand. Then the energy index of reliability can be defined as EIR:

$$EIR = 1 - LOEE_{p.u.} \tag{3.6}$$

The LOLE method is the most widely used probabilistic reliability evaluation method, however there are also more indices which based on different factors and calculation procedures. The basic indices like LOLE and LOEE can indicate the adequacy of system, which are based on the system configurations like the generating units size, availability, load demand and uncertain factors.

3.2 Reliability analysis of generating system with sequential MCS method

For the reliability analysis of generating system, the most important part is modeling the status of generation units. In the most common two-state model, the unavailability probability, which is often known as the unit forced outage rate (FOR) is used to model the status. So a random numerous with the range of [0,1] will be generated, if the number is bigger than the UCR, then this status is taken as available, otherwise the unit is deemed as the down state.

In the sequential MCS, the mere knowledge about the status of units is not enough, the durations of status are also needed. So the random values of time to repair (TTR) and time to failure (TTF) are defined as:

$$TTR = -\frac{lnR_1}{\mu} \tag{3.7}$$

$$TTF = -\frac{lnR_2}{\lambda} \tag{3.8}$$

where R_1 and R_2 are random numbers between [0,1], μ and λ are expected repair and failure rate.

So with the status and duration time of different units known, the combination of different units' status with a time based sequential method can give a precise picture of the whole system status, just like the Figure 3.4 shows. With the generating system status known, the reliability index like LOLE can be calculated in combination with a specific load model, the whole simulation procedures including following steps:

1. Set N as the total number of years for simulation, i as the number of year sampled, initialize $i = 0$.

2. Consider the sample year $i = i + 1$.

3. Generate the state sequence for each unit during the sample year i using the methods introduced above, combine the status of units to generate the available generating capacity sequence in the sample year.

4. Compare the generating capacity sequence with the chronological load sequence, count the number of days or hours d_i on which the load exceeds the available generating capacity.

5. Update the total number of days or hours of loss of load, $D = D + d_i$.

6. Calculate the updated value of $LOLE = D/i$.

7. Repeat the step 1-6 above until $i = N$ or the acceptable value of $LOLE$ is reached.

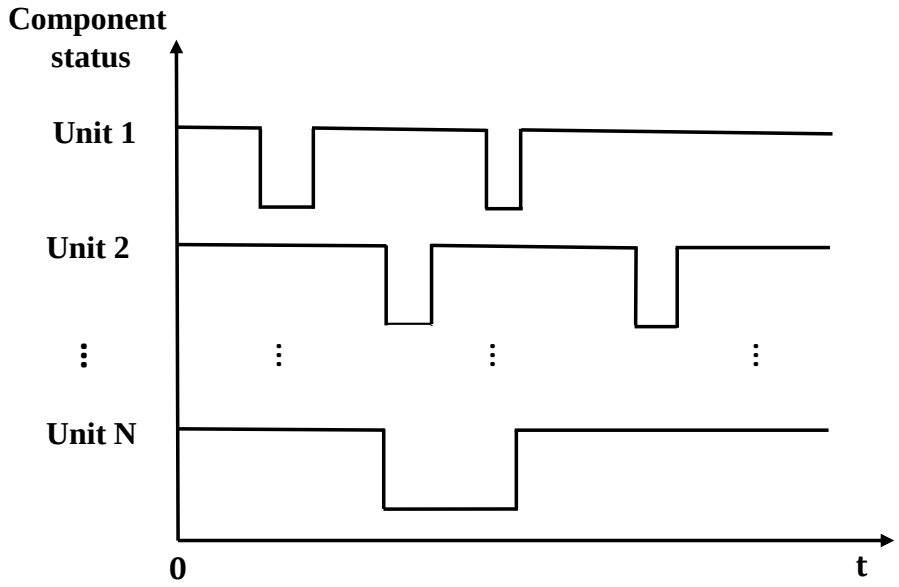

Figure 3.4: The combination of component status in a sequential method

3.3 The effect of EV charging on power system reliability

The reliability test system such as Roy Billinton Test system (RBTS) and IEEE Reliability Test System (RTS) have been widely used as a benchmark case to show the reliability assessment outcomes and development in the probabilistic reliability evaluation methods. The RBTS system was first put forward by Dr. Roy Billinton [67] in 1989, it have 6 buses and 11 generators, the transmission system voltage is 230 kV, the total installed generating capacity is 240 MW and the system peak load is 185 MW. Compared with the RTS,the system size is relatively small, so it's very easy to modify the test system. The system structure is shown in Figure 3.5.

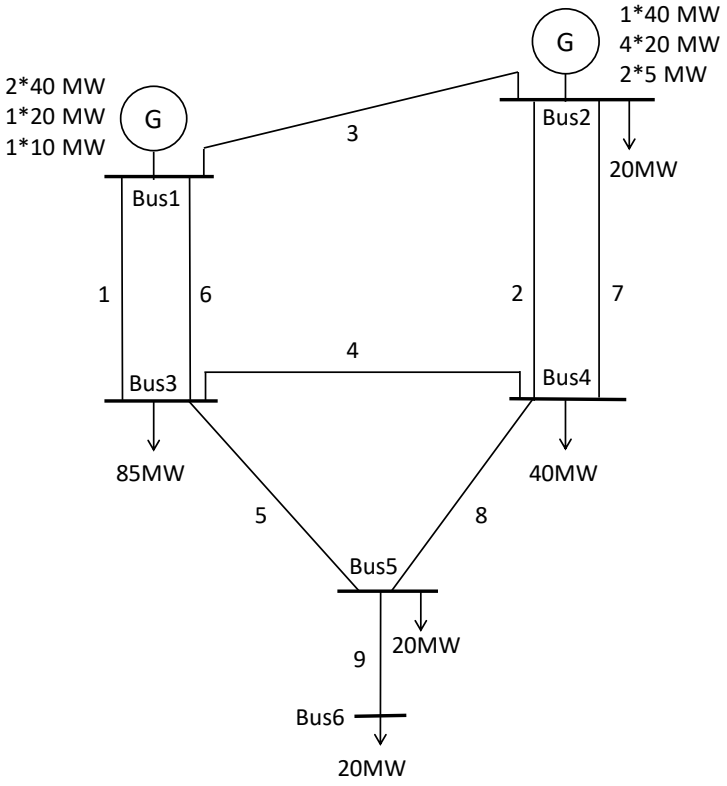

Figure 3.5: 6 Bus Roy Billinton Test system [67]

The reliability data of generating units in the RBTS system is shown in Table 3.1. Because the sequential MCS method is used in this research, so except for the generating system, a typical sequential load model is also needed, it is constructed in this research by modifying the load model in [68]. The characteristics of this load model are shown in Table 3.2, 3.3, 3.4.

Table 3.1: Reliability indexes of generating units in RBTS [67].

Unit Size	**Unit Type**	**Unit Number**	**FOR**	**MTTF**	**Failure rate per year**	**MTTR**	**Repair rate per year**	**Scheduled maintenance(wk/yr)**
5	Hydro	2	0.010	4380	2.0	45	198.0	2
10	Thermal	1	0.020	2190	4.0	45	196.0	2
20	Hydro	4	0.015	3650	2.4	45	157.0	2
20	Thermal	1	0.025	1752	5.0	45	195.0	2
40	Hydro	1	0.020	2920	3.0	45	147.0	2
40	Thermal	2	0.030	1460	6.0	45	194.0	2

Table 3.2: Weekly peak load as a percentage of annual peak load [67].

Week	**Peak Load (%)**	**Week**	**Peak Load (%)**	**Week**	**Peak Load (%)**	**Week**	**Peak Load (%)**
1	86.2	14	75.0	27	75.5	40	72.4
2	90.0	15	72.1	28	81.6	41	74.3
3	87.8	16	80.0	29	80.1	42	74.4
4	83.4	17	75.4	30	88.0	43	80.0
5	88.0	18	83.7	31	72.2	44	88.1
6	84.1	19	87.0	32	77.6	45	88.5
7	83.2	20	88.0	33	80.0	46	90.9
8	80.6	21	85.6	34	72.9	47	94.0
9	74.0	22	81.1	35	72.6	48	89.0
10	73.7	23	90.0	36	70.5	49	94.2
11	71.5	24	88.7	37	78.0	50	97.0
12	72.7	25	89.6	38	69.5	51	100.0
13	70.4	26	86.1	39	72.4	52	95.2

Table 3.3: Daily peak load as a percentage of weekly peak load [67].

Day	1	2	3	4	5	6	7
Peak load(%)	93	100	98	96	94	77	75

Table 3.4: Hourly peak load as a percentage of daily peak load [67].

	Winter weeks 1-8 & 44-52		Summer weeks 18-30		Spring/Fall weeks 9-17 & 31-43	
Hour	Weekday	Weekend	Weekday	Weekend	Weekday	Weekend
1	67	78	64	74	63	75
2	63	72	60	70	62	73
3	60	68	58	66	60	69
4	59	66	56	65	58	66
5	59	64	56	64	59	65
6	60	65	58	62	65	65
7	74	66	64	62	72	68
8	86	70	76	66	85	74
9	95	80	87	81	95	83
10	96	88	95	86	99	89
11	96	90	99	91	100	92
12	95	91	100	93	99	94
13	95	90	99	93	93	91
14	95	88	100	92	92	90
15	93	87	100	91	90	90
16	94	87	97	91	88	86
17	99	91	96	92	90	85
18	100	100	96	94	92	88
19	100	99	93	95	96	92
20	96	97	92	95	98	100
21	91	94	92	100	96	97
22	83	92	93	93	90	95
23	73	87	87	88	80	90
24	63	81	72	80	70	85

The load variation is also shown in Figure 3.6, the yearly peak load 185 MW appears at winter, near the end of the year.

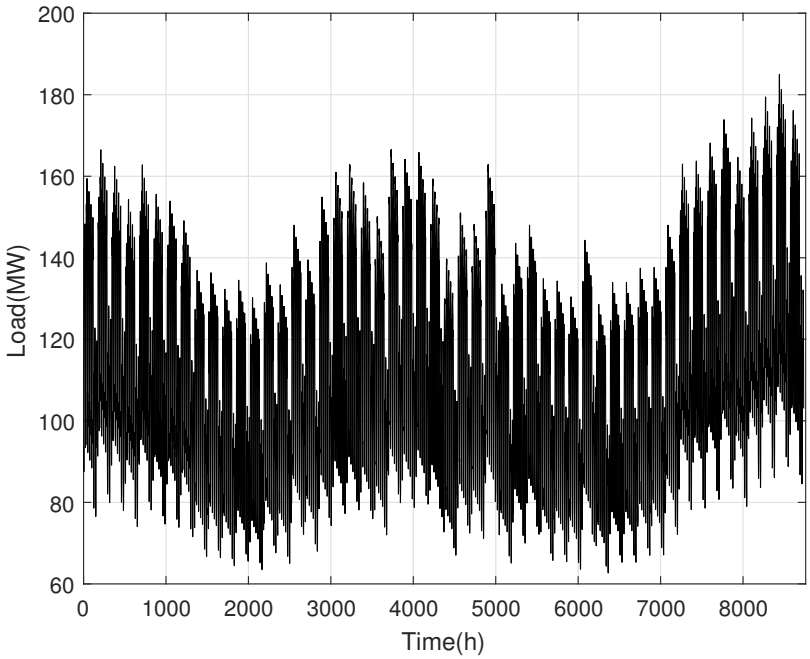

Figure 3.6: Load variation of the test system in a year

The EV charging load in Chapter 2 is calculated based on the real world transportation survey, which includes both the transportation and charging characteristics of electric vehicles. So the charging loads of 3000 EVs are added into the RBTS system to evaluate its effect on power system reliability in the planning phase, the influence is shown in Table 3.5. The results show the uncontrolled charging of EV will decrease the reliability of the system and the smart charging can mitigate the detrimental effects.

Table 3.5: Reliability index of the test system under different load scenarios.

Reliability index	System base load	Baseload+Uncontrolled Charging load	Baseload+Smart Charging load
LOLE	1.1010	1.3140	1.2340

Chapter 4

Power system reliability analysis with EV providing operating reserve

The reliability analysis of power system can be divided into two different time spans. Chapter 3 focus on analyzing the effects of large scale integration of EV on reliability in planning phase. This chapter focus on the effects on reliability in operating phase, the mechanism of EV providing operating reserve and its effects on reliability will be comprehensively discussed.

4.1 Operating reserve

In order to keep the safe and reliable operation of power system, the production and consumption of electric power must be instantaneously balanced all the time. However, with the increasing integration ratio of renewable energy, the stochastic nature of renewable energy makes the generating system faces great uncertainty. Meantime the demand of electric power is also uncertain. The most reasonable method in counter with the uncertainty is to keep some level of margins between the generating

capacity and expected load. So the system can deal with the uncertainty and unexpected contingencies in both generation and load side. This margin is often called operating reserve, which is usually provided by stand by units.

For the power system operation, system operators will make unit commitment decisions according to the generating units merit orders or the market bids, and the decisions will be modified with the latest system information using the methods like economic dispatch. There are basically several different balance strategies that have different time frames [69]. The forward scheduling and unit commitments are meant to meet the general load pattern of a day. Load following is used to follow the load variation trend in the day, which is usually performed in the method of starting or shutting quick start units or hydro units according to the economic dispatch signals. The regulation is used ot balance the fast minutes' or seconds' level load or generation variation. All these measures work together to in contour with all the variation and forest errors and achieve the balance.

During a contingency like loss of generation units, the reserve or additional supply need to respond to the disturbance immediately. A number of different reserves and resources will response in different time. First, the loss of a generator will break the balance, then the synchronous generators will slow down their rotational speeds and then comes with the system frequency decline, the system inertia will slow the drop. Meantime the governor on the generator will automatically responds to the frequency deviation. Both the spinning reserve and non-spinning reserve are deployed to fill the gap, the load side can also respond through the demand side management. Lastly, the supplemental reserves are deployed to allow the fast speed and expensive responses to be restored just in case of a subsequent event. The whole process is shown in Figure 4.1. The over-frequency events, though rare, can be responded in similar methods.

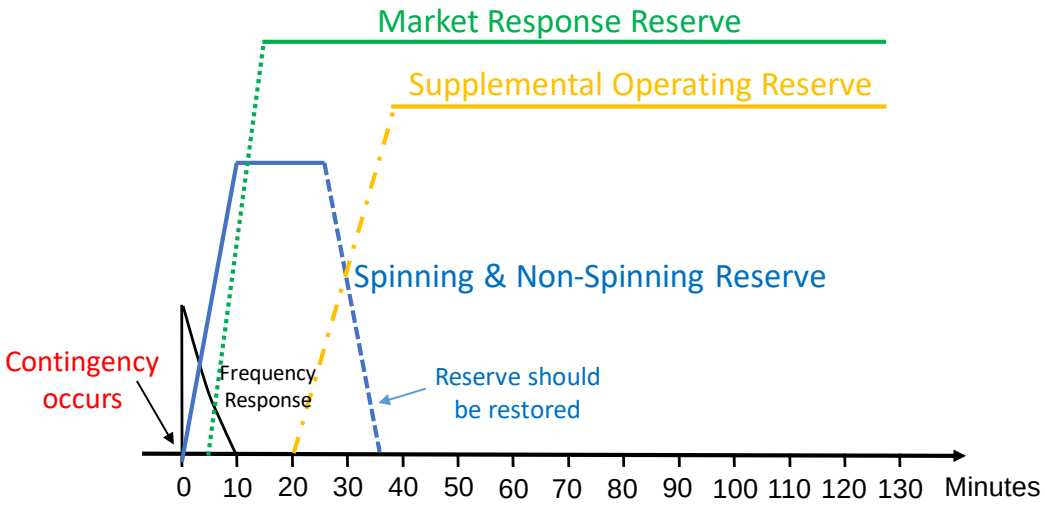

Figure 4.1: The response of reserves in a contingency event.

In the view of power system operation, the operating reserve can be divided into several different categories according to their response speeds, durations and frequencies. Some operating reserves are used to deal with the daily variation, while some may only be needed for the rare unexpected contingencie, like loss of a generator. So the reserve can be divided as no-event or event based, events means scenarios that are rarely happeded but have severe effect. For the events, the operating reserve can also be called contingency reserve, which is mainly used for power balancing under infrequent but severe events. Both the spinning and non-spinning reserve can be contingency reserve. Different kinds of generator units and responsive loads are better at providing different kinds of operating reserve according to their characteristics. For the conventional thermal units, the amounts of spinning reserve they can provide are limited by their ramp rates. The nuclear units normally don't provide operating reserve. Some gas fired combustion engines and fast response hydro units can provide some non-spinning reserve. However, for both the large thermal plants and combustion engines that operating at their maximum efficiency status, the amounts of operating reserve they can provide are greatly limited.

In fact, with some well designed market mechanism, the load side can be a ideal provider for operating reserve. The demand side management can provide different types of operating reserve and normally has a very fast response speed. The flexibility of EV and its special characteristics of energy storage making it proper for providing all kinds of ancillary services and reserves. The fundamental meanings of reserve are analyzed in [70], which are from the perspective of flexibility. It's similar with the idea in this research, which the flexibility of EV is taken as resources and used to provide reserve for the power system. Meanwhile, the research in [71] showed operating reserve has a substantial impact on the installed power system generation capacity and operation. With enough operating reserve, the system can have a substantial decrease in the cost of renewable energy integration.

Based on these characteristics, this chapter focus on the mechanism of aggregated EVs providing operating reserve, more precisely contingency reserv, and its effects on power system reliability. For EVs, most time there are no real energy exchanges because of the provided operating reserve, the reserve capacity will only be called for the rare and severe events. EVs will get revenues for their provided capacities, and there will have extra compensations if they are called and deployed. For the non-event based cases, the regulation reserve can also be provided by EVs, which is not a main concern in this research.

4.2 PJM and Modified PJM method for unit commitment risk analysis

It's important for utilities to determine a reasonable amount of operating reserve that could achieve the delicate balance between reliability and cost. Historically, the empirical rule-of-thumb methods are used. Usually the operating reserve capacity is set to equal with the capacity of the largest unit. The deterministic method ignores

the probabilistic nature of the system behaviors and component failures, with an increasing integration ratio of renewable energy, the traditional empirical method could cause over-scheduling or under-scheduling problems, which will affect the economical and reliable operation of power system.

A lot of literatures [72, 73, 74] focusing on the economic aspects of the units commitment and the associated unit commitment risks are rarely evaluated. So the probabilistic methods that could provide a risk index to enable making comparisons between different system operating scenarios are necessary. In this research, the unit commitment risk is used to measure the reliability. With an acceptable risk level, the utilities can schedule the generating units in the most economical methods.

The PJM method [64] was firstly proposed for the evaluation of spinning reserve need of Pennsylvania-New Jersey-Maryland (PJM) system. The basic idea of PJM method is to measure the probability that the committed generation units just satisfying or failing to satisfy the demand said need during a period of time that no replacements are available. So this reliability index can be continuously re-evaluated through the whole time as the status of loads and generating system change.

If the same two-state model is used to represent the generating units, assuming this unit is working normally at $t = 0$, then the possibility of a unit in failure statue during the time T can be expressed as:

$$P\left(failure\right) = \frac{\lambda}{\lambda + \mu} - \frac{\lambda}{\lambda + \mu} e^{-(\lambda+\mu)T} \tag{4.1}$$

If the repair or replacement are neglected during the T, μ is 0, then the Equation 4.1 is simplified as:

$$P\left(failure\right) = 1 - e^{-\lambda T} \tag{4.2}$$

Because the λ for a generating unit is very small, so for a short lead time of several hours, the $\lambda T \ll 1$ is usually true, then:

$$P\left(failure\right) \simeq \lambda T \tag{4.3}$$

Equation 4.3 stands for the failure probability of a unit during the lead time T with no repair or replacement, it's also called outage replacement rate (ORR). The ORR is similar with the FOR used in the planning phase reliability analysis in Chapter 3, however the ORR is a time dependent variable.

The loads are assumed to be constant during the lead time in PJM method, therefore the unit commitment risk values can be directly deduced from the COPT of generating system and load. The modified PJM method taking the standby units into the unit commitment risk analysis, both the start-up and operation failures of standby units are considered, which means the standby units may fail to start during their lead time and may suffer failures after their lead time. One visual and convenient method to show the risk is using the area risk curve [75].

For a two-state unit model defined in Equation 4.2, the risk density function of this model is:

$$f\left(Risk\right) = \frac{dp}{dt} = \lambda e^{-\lambda t} \tag{4.4}$$

The probability of a unit fails in the period of $(0, T)$ is:

$$P\left(0, T\right) = \int_{0}^{T} \lambda e^{-\lambda t} dt \tag{4.5}$$

With the modified PJM method, the system's unit commitment risk evaluation can be divided into several different parts, like the Figure 4.2 shows, the total risk is the sum of $R_a\left(0, T_1\right)$, $R_b\left(T_1, T_2\right)$ and $R_c\left(T_2, T_3\right)$.

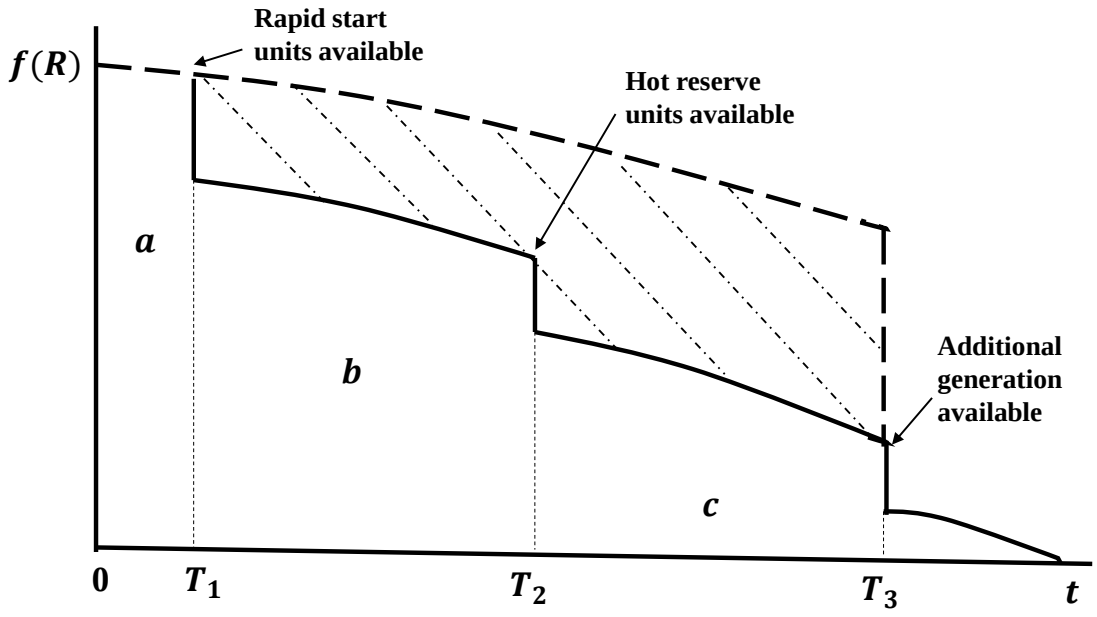

Figure 4.2: Area risk curve of the system.

4.3 Capacity estimation of EV providing operating reserve

The V2G enabled smart charging model in Chapter 2, Section 4 is used for the EV charging control in this section. It should emphasized that providing operating reserve doesn't affect the normal daily operation of EV, because the operating reserve will only be called for serious contingencies in power system, which usually have low probability but high risk. So for the EV that providing operating reserve, in most time it only provides an available capacity, there is no real energy exchange because of the provided reserve.

As discussed before, the V2G enabled smart charging algorithm control the behaviors of EV at three different status: charging, discharging and idle, the control sequence for EV i during the connected period is expressed as:

$$\boldsymbol{K_i} = \left[K_i^{t_{in}}, \cdots K_i^t \cdots K_i^{t_{out}}\right] \tag{4.6}$$

where K_i^t=1 means the i_{th} EV is charging at time t, $K_i^t = -1$ means the i_{th} EV is discharging at time t and K_i^t=0 means the EV is in idle status.

The status vectors $\boldsymbol{C_i}$ and $\boldsymbol{I_i}$ are used to separately indicate the charging and idle status of each vehicle, which are defined as:

$$\boldsymbol{C_i} = \left[C_i^{t_{in}}, \cdots C_i^t, \cdots C_i^{t_{out}}\right],\ C_i^t = \begin{cases} 1, & if\ k_i^t = 1 \\ 0, & otherwise \end{cases} \tag{4.7}$$

$$\boldsymbol{I_i} = \left[I_i^{t_{in}}, \cdots I_i^t, \cdots I_i^{t_{out}}\right],\ I_i^t = \begin{cases} 1, & if\ k_i^t = 0 \\ 0, & otherwise \end{cases} \tag{4.8}$$

4.3.1 Interruptible charging capacity

A new status vector $\boldsymbol{A_i}$ is defined to indicate the charging status of the i_{th} in a two days' research period.

$$\boldsymbol{A_i} = \left[A_i^0, \cdots A_i^t, \cdots A_i^{48}\right],\ A_i^t = \begin{cases} 1, & if\ C_i^t = 1 \\ 0, & otherwise \end{cases} \tag{4.9}$$

The energy losses of i_{th} EV due to the interruption of existing charging schedule is defined as:

$$E_{L,i} = \sum_{t=t_{Is}}^{t_{Is}+t_{Id}} P_i \boldsymbol{A_i} \tag{4.10}$$

where t_{Is} is the starting time point of charging interruption, t_{Id} is the duration of interruption, P_i is the charging rate.

If the interruption happens, although it's a very rare case, the existing EV charging schedule will be interrupted. The EV should has enough time to compensate the energy losses and meets its initial set point of energy need, the energy compensated

during the connected time after the interruption can be defied as:

$$E_{C,i} = \sum_{t_{Is}+t_{Id}}^{t_{i,out}} P_i \; t \tag{4.11}$$

In the real world application, there will have specific economic compensations for the interruption, so the cost increase that because of the deviation of existing optimal charging schedule will not be a problem.

The interruptible energy of i_{th} EV during the interruption duration t_{Id} is:

$$E_{I,i} = min\left(E_{L,i}, E_{C,i}\right) \tag{4.12}$$

So the total interruptible capacity of all controlled EVs is:

$$P_I = \sum_{i=1}^{n} \frac{E_{I,i}}{t_{Id}} \tag{4.13}$$

4.3.2 V2G capacity

A new status vector $\boldsymbol{V_i}$ is defined to indicate whether the i_{th} EV in idle state and provides V2G capacity in a two days' research period.

$$\boldsymbol{V_i} = \left[V_i^0, \cdots V_i^t, \cdots V_i^{48}\right], \; V_i^t = \begin{cases} 1, & if \; I_i^t = 1 \\ 0, & otherwise \end{cases} \tag{4.14}$$

The energy losses of i_{th} EV due to the status transfer form idle to discharging is defined as:

$$E_{L,i} = \sum_{t=t_{Vs}}^{t_{Vs}+t_{Vd}} D_i \boldsymbol{V_i} \tag{4.15}$$

where t_{Vs} is the starting time point of providing V2G capacity, t_{Vd} is the duration time, D_i is the discharging rate.

Similar with the interruption scenario, the energy compensated during the connected time after the interruption can be defied as:

$$E_{C,i} = \sum_{t_{Vs}+t_{Vd}}^{t_{i,out}} D_i \; t \tag{4.16}$$

The total discharging energy of i_{th} EV during t_{Vd} is:

$$E_{V,i} = min\left(E_{L,i}, E_{C,i}\right) \tag{4.17}$$

So the total V2G capacity of all controlled EVs is:

$$P_V = \sum_{i=1}^{n} \frac{E_{V,i}}{t_{Vd}} \tag{4.18}$$

4.4 Analysis procedures

Step 1: Set the lead time of the system, then calculate the outage replacement rate (ORR) of each generating units using Equation 4.3.

Step 2: Calculate the capacity outage probability table (COPT) of generating system, combined with the corresponding load and using the PJM method in Section 2 to get the original unit commitment risk (UCR).

Step 3: Collect information about EVs' original charging schedules, obtain $\boldsymbol{A_i}$, $\boldsymbol{V_i}$.

Step 4: Calculate P_I and P_V using the methods introduced in Section 3.

Step 5: Model the operating reserve provided by aggregated EVs as a four-state rapid start unit, set the related lead time and use the modified PJM method to calculate the corresponding unit commitment risk (UCR).

4.5 Numerical study

As introduced before, this chapter focus on the effects of EV providing operating reserve on power system reliability in the operation phase, so a test system which based on RBTS system is designed. A representatives day is choose as base case, the base load is shown in Figure 4.3. The priority loading order in RBTS is used in this research to arrange the generating unit schedule, which is shown in Table 4.1.

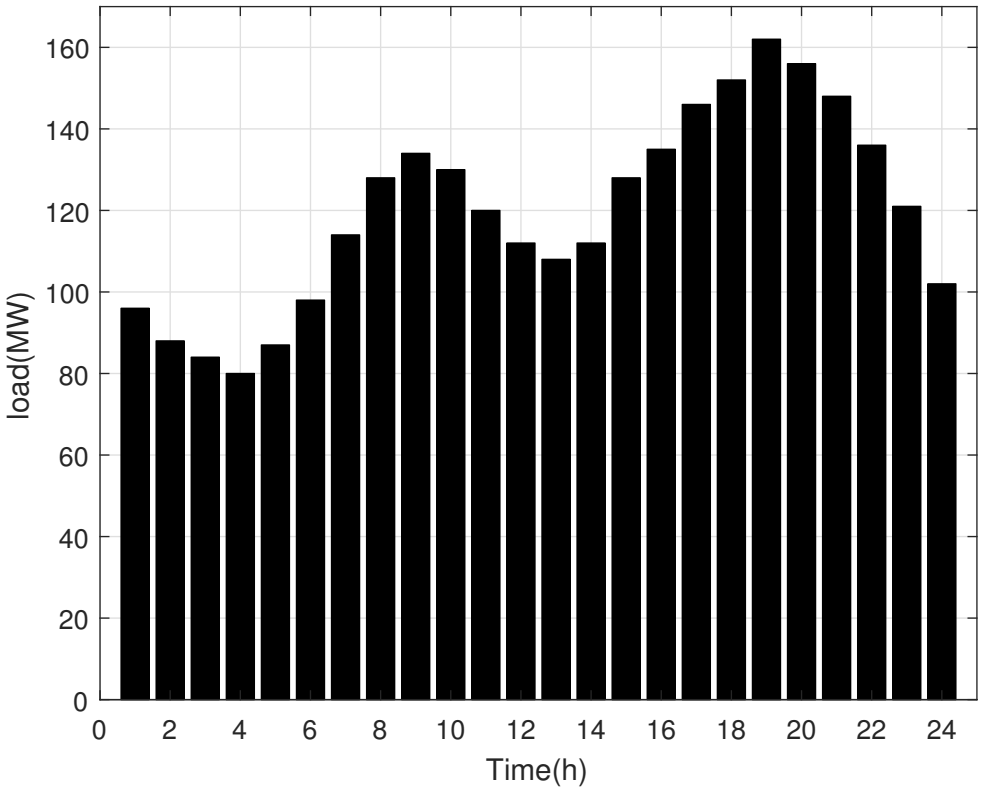

Figure 4.3: System base load of the designed test system.

The lead time of the system is set as one hour. According to the first two steps in analysis procedures introduced in Section 4.4, the capacity outage probability table (COPT) of 7 scheduled units for the peak load hour at 9 pm is shown in Table 4.2. Combine the COPT with system load of 162 MW, the unit commitment risk (UCR) at this period can be get as 0.00282781, similarly each hour's UCR can be calculated, the results are shown in Table 4.3.

Table 4.1: RBTS priority loading order.

Priority loading order	**Unit size(MW)**	**Type**	**Failure rate (failures per year)**
1	40	Hydro	3
2-3	20	Hydro	2.4
4-5	40	Thermal	6
6	20	Thermal	5
7	10	Thermal	4
8-9	20	Hydro	2.4
10-11	5	Hydro	2

Table 4.2: COPT for the scheduled 7 generating units.

Capacity out (MW)	**Capacity in (MW)**	**Probability**	**Cumulative Probability**
0	190	0.99671686	1.00000000
10	180	0.00045533	0.00328314
20	170	0.00111552	0.00282781
30	160	0.00000051	0.00171229
40	150	0.00170815	0.00171178
50	140	0.00000078	0.00000363
60	130	0.00000191	0.00000285
70	120	0.00000000	0.00000094
80	110	0.00000094	0.00000094
90	100	0.00000000	0.00000000
100	90	0.00000000	0.00000000

The operating reserve capacity an EV aggregator (3000 EVs) can provide is calculated based on the methods introduced in Section 4.3. The parameters of electric vehicles are same as in Chapter 2, the charging and discharging rate of EV is set as 3.3 kW. EV providing operating reserve in most time is just providing an available capacity, there is no related energy exchange. Although there will have some revenues, each EV should focus on optimizing its charging schedule to minimize the total cost, so the V2G enabled smart charging algorithm is used in this case study to optimize the charging behaviors of EV. Then the available capacity for providing operating reserve is calculated based on the optimized charging schedules.

Table 4.3: Test system design and initial unit commitment risk.

Hour	**Load**	**Units Number**	**Generating Capacity**	**Unit Commitment Risk**
1	96	4	120	0.00157447008740850
2	88	4	120	0.00157447008740850
3	84	4	120	0.00157447008740850
4	80	4	120	0.00102723767857720
5	87	4	120	0.00157447008740850
6	98	4	120	0.00157447008740850
7	114	5	160	0.00171146559797494
8	128	5	160	0.00225832319008786
9	134	5	160	0.00225832319008786
10	130	5	160	0.00225832319008786
11	120	5	160	0.00171146559797494
12	112	5	160	0.00171146559797494
13	108	5	160	0.00171146559797494
14	112	5	160	0.00171146559797494
15	128	5	160	0.00225832319008786
16	135	6	180	0.00171177773130377
17	146	6	180	0.00282781044854103
18	152	6	180	0.00282781044854103
19	162	7	190	0.00282781044854103
20	156	6	180	0.00282781044854103
21	148	6	180	0.00282781044854103
22	136	6	180	0.00171177773130377
23	121	5	160	0.00225832319008786
24	102	5	160	0.00171146559797494

If considering the system's safe operation, the status of EV can't change from charging to idle then discharging, the capacity of operating reserve an EV aggregator can provide in the test day is shown in Figure 4.4(a). If status switch is allowed, then the available reserve capacity is shown in Figure 4.4(b).

The results show the available operating reserve capacity this EV aggregator can provide mainly concentrate on te load valley hours. It is because this aggregator's control area is a residential area, most of charging behaviors happened at night hours, besides the smart charging algorithm transfer huge amount of charging load from peak load hours to the night valley hours. The permission of direct switching from

charging status to discharging status can greatly increase the available operating reserve capacity, however, the power flow reversal caused by large scale distributed discharging should be carefully evaluated by both the aggregators and DSOs in case endanger the safe operation of power system.

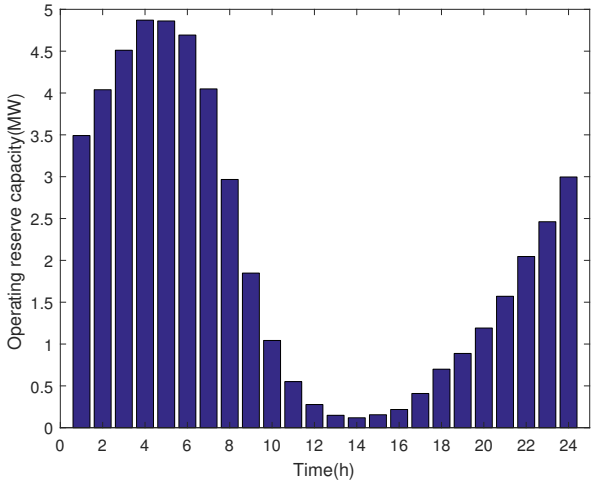

(a) Mehtod 1.

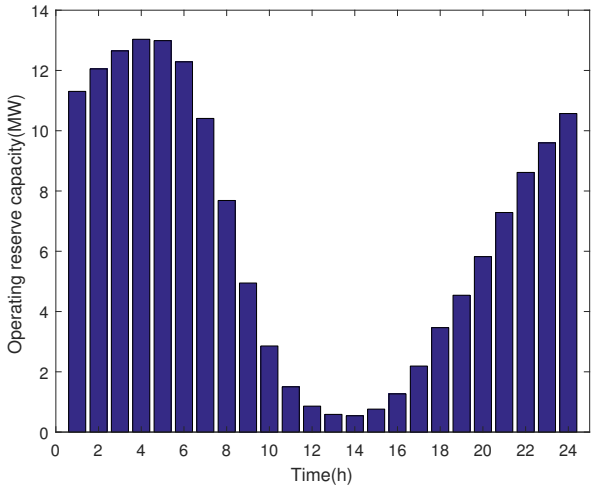

(b) Mehtod 2.

Figure 4.4: Operating reserve capacity provided by 3000 EVs in test day.

The operating reserve provided by the EV aggregator is modeled as an equivalent rapid start unit as the Step 5 in analysis procedures. In order to accurately model the response characteristics, the rapid start unit is modeled as a four-state model, which is shown in Figure 4.5. The parameters of this rapid unit are shown in

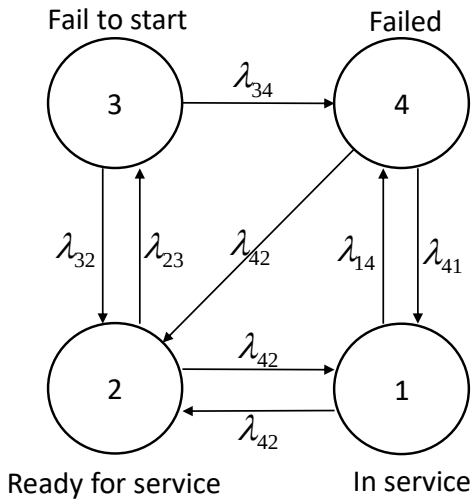

Figure 4.5: Four-state representative model of the rapid start unit.

Table 4.4. For the market based mechanism, there need some time for the contracting between different market players and safety evaluation, so the lead time of the rapid start unit is set as 5 minutes.

Table 4.4: Status transition parameters of equivalent rapid start unit.

λ_{11}=0	λ_{12}=0.0050	λ_{13}=0	λ_{14}=0.0010
λ_{21}=0.0033	λ_{22}=0	λ_{23}=0.0001	λ_{24}=0
λ_{31}=0	λ_{32}=0	λ_{33}=0	λ_{34}=0.0250
λ_{41}=0.0150	λ_{42}=0.0250	λ_{43}=0	λ_{44}=0

According with the modified PJM method introduced in Section 4.2, the system unit commitment risks with or without additional market acquired operating reserve in the test day can be calculated, the results are shown in Figure 4.6. The different scenarios show the discrete nature of the UCR, which is caused by the discrete change of generating capacity in the power system operation. The numerical results show the operating reserve provided by aggregated EVs can reduce the system unit commitment risk. For the test system, acquiring more than 20MW operating reserve on the reserve market can greatly reduce the system risk.

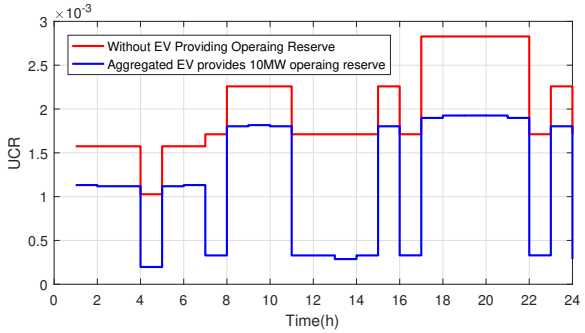

(a) 10MW reserve purchased from aggregators.

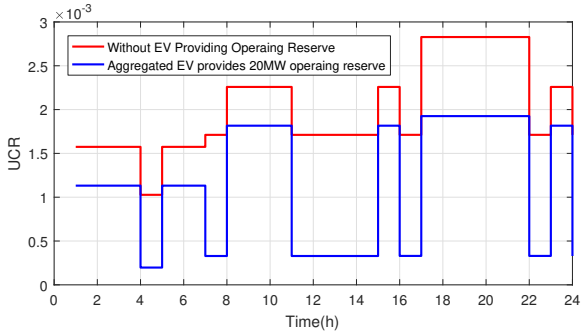

(b) 20MW reserve purchased from aggregators.

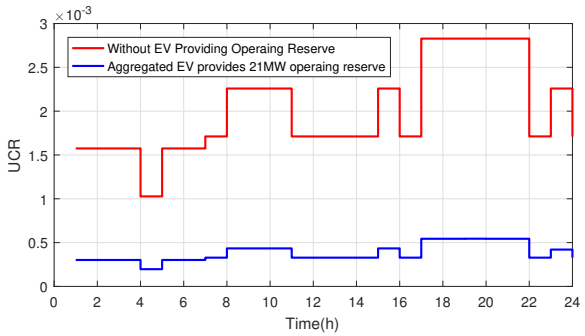

(c) 21MW reserve purchased from aggregators.

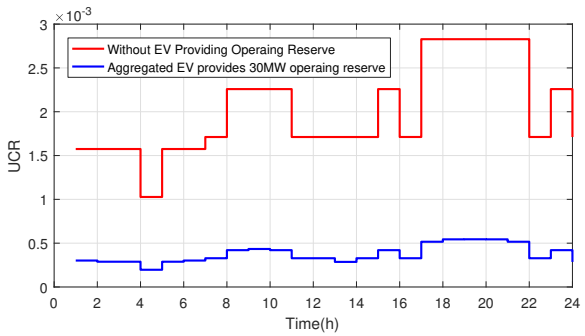

(d) 30MW reserve purchased from aggregators.

Figure 4.6: System UCR with different capacities of additional operating reserve

Chapter 5

Conclusion and future work

With the increasing integration level of electric vehicles into the grid, this research shows the uncoordinated charging of EVs will greatly increase the system peak load, which will have a significant effect on the safe and reliable operation of the power system.

The existing smart charging control algorithms are analyzed in detail and categorized as distributed and centralized methods. Based on these categories, two smart charging algorithms are put forward and evaluated in this research. The distributed smart charging algorithm is based on the multi-agent system. Each EV agent optimizes its own charging schedule according to the charging price signal from the aggregator agent. The smart charging pricing and sequential price update mechanism have been proven useful and can greatly decrease the computation complexity and communication burden. The binary hybrid PSO-GSA method is proved to be able to find the optimal point accurately and rapidly. The V2G enabled smart charging algorithm uses the centralized method. In order to relieve the computation burden and curse of dimensionality, the dominant solution matrix is used in this smart PSO optimization algorithm, so the search space can be reduced to a reasonable range.

Both the smart charging algorithms are proven to be effective in flattening the load curve and transferring the charging load to the night valley hours in the case studies.

Integration of EV charging load into the power system reliability analysis framework offers a new perspective in the evaluation and analysis of smart charging algorithms. The analysis results about the effects on power system reliability show the importance of smart charging control, the results also show the existing power system reliability methods should be modified to be able to include the smart grid elements, like electric vehicles, wind power, energy storage systems, etc.

The flexibility and energy storage characteristics of electric vehicles make it possible to provide operating reserve for the power system. The method for estimating the available reserve capacity in this research is based on two different aspects. EVs' charging load can be taken as interruptible loads when calculate the interruptible capacity, the batteries can be taken as energy storage systems in V2G mode when calculate the V2G capacity. By modeling the operating reserve as a rapid start unit and using the modified PJM method, this approach has been proven to be very effective in the power system reliability analysis during the operating phase and has a remarkable effect on the reduction of unit commitment risk.

The service market of EV charging is gradually formed, the independent third party market role like aggregator will coordinate the distributed and stochastic charging behaviors of large amount of electric vehicles. In the meantime, with the development of communication and intelligence technologies, aggregator can collect the real time data about EVs' driving patterns, charging needs, battery status, etc. By analyzing huge amounts of collected data, the aggregator can have an accurate perception of the system status and make precise predictions about the future's energy needs. By continually learning each end user's transportation and energy use pattern, the aggregator can work more efficiently. These information will also support its biddings in both energy and ancillary service market. How to enable the aggregator

with self-learning ability and how to make optimal biddings in a deregulated market are important parts of future work.

In a market based control architecture, the relations between EVs, aggragators, DSOs and TSOs should be carefully analyzed. The complex and sometimes conflicting relations will be evaluated in future work, the game theory and multi-agent system are promising solutions. The non-cooperative game theory has been proven to be able to accurately model the competitive relations between aggregators, the Nash Equilibrium of the game is the balance status in the market. However, there are also potential cooperations in the system, the combination of cooperative game and non-cooperative game is also a part of future work.

The smart charging control of electric vehicles could also be coordinated with the renewable energy integration, especially with the wind power. The energy storage ability and the flexibility in charging scheduling might become the solutions for renewable energy's intermittency. Meantime, the system operator and planner can have a more precise knowledge about the reliability status of the system by adding both the renewable energy and electric vehicles into the power system reliability analysis, which can not only ensure the safe and reliable operation of the system but also help make more economical investment decisions.

And there are also more potential applications for aggregated EVs, such as frequency regulation. The EV aggregator's role can also be extended as a comprehensive demand side resources aggregator, which aggregate different kinds of controllable demand side resources like electric vehicles, HAVC, water heater. Then, it can bargain in both the energy and ancillary service market and earn revenues by providing all kinds of valuable aggregated demand side response resources.

Bibliography

[1] "Technology roadmap: Electric and plug-in hybrid electric vehicles(EV/PHEV)." http://www.iea.org/publications/freepublications/publication.html.

[2] "Electric Drive Sales." http://electricdrive.org/index.php?ht=d/sp/i/20952/pid/20952.

[3] "Electric Vehicles (EVs, HEVs, PHEVs)." http://www.in.gov/oed/2675.htm.

[4] X. Fang, S. Misra, G. Xue, and D. Yang, "Smart gridthe new and improved power grid: A survey," *IEEE communications surveys & tutorials*, vol. 14, no. 4, pp. 944–980, 2012.

[5] S. Han, S. Han, and K. Sezaki, "Development of an Optimal Vehicle-to-Grid Aggregator for Frequency Regulation," *IEEE Transactions on Smart Grid*, vol. 1, pp. 65–72, June 2010.

[6] K. Jorgensen, "Technologies for electric, hybrid and hydrogen vehicles: Electricity from renewable energy sources in transport," *Utilities Policy*, vol. 16, pp. 72–79, June 2008.

[7] S. Han and S. Han, "Economics of V2G frequency regulation in consideration of the battery wear," in *2012 3rd IEEE PES Innovative Smart Grid Technologies Europe (ISGT Europe)*, pp. 1–8, Oct. 2012.

[8] J. Y. Yong, V. K. Ramachandaramurthy, K. M. Tan, and N. Mithulananthan, "A review on the state-of-the-art technologies of electric vehicle, its impacts and prospects," *Renewable and Sustainable Energy Reviews*, vol. 49, pp. 365–385, Sept. 2015.

[9] Y. J. Kim, G. Del-Rosario-Calaf, and L. K. Norford, "Analysis and Experimental Implementation of Grid Frequency Regulation using Behind-the-Meter Batteries Compensating for Fast Load Demand Variations," *IEEE Transactions on Power Systems*, vol. PP, no. 99, pp. 1–1, 2016.

[10] J. Aghaei, A. E. Nezhad, A. Rabiee, and E. Rahimi, "Contribution of Plug-in Hybrid Electric Vehicles in power system uncertainty management," *Renewable and Sustainable Energy Reviews*, vol. 59, pp. 450–458, June 2016.

[11] R. Sioshansi and P. Denholm, "The Value of Plug-In Hybrid Electric Vehicles as Grid Resources," *Energy Journal*, vol. 31, pp. 1–23, July 2010.

[12] J. D. Kim and M. Rahimi, "Future energy loads for a large-scale adoption of electric vehicles in the city of Los Angeles: Impacts on greenhouse gas (GHG) emissions," *Energy Policy*, vol. 73, pp. 620–630, Oct. 2014.

[13] T. Donateo, F. Ingrosso, F. Licci, and D. Laforgia, "A method to estimate the environmental impact of an electric city car during six months of testing in an Italian city," *Journal of Power Sources*, vol. 270, pp. 487–498, Dec. 2014.

[14] W. Ke, S. Zhang, X. He, Y. Wu, and J. Hao, "Well-to-wheels energy consumption and emissions of electric vehicles: Mid-term implications from real-world features and air pollution control progress," *Applied Energy*, vol. 188, pp. 367–377, Feb. 2017.

[15] E. A. Nanaki and C. J. Koroneos, "Comparative economic and environmental analysis of conventional, hybrid and electric vehicles – the case study of Greece," *Journal of Cleaner Production*, vol. 53, pp. 261–266, Aug. 2013.

[16] E. A. Nanaki and C. J. Koroneos, "Climate change mitigation and deployment of electric vehicles in urban areas," *Renewable Energy*, vol. 99, pp. 1153–1160, Dec. 2016.

[17] D. McCarthy and P. Wolfs, "The HV system impacts of large scale electric vehicle deployments in a metropolitan area," in *2010 20th Australasian Universities Power Engineering Conference*, pp. 1–6, Dec. 2010.

[18] T. K. Kristoffersen, K. Capion, and P. Meibom, "Optimal charging of electric drive vehicles in a market environment," *Applied Energy*, vol. 88, pp. 1940–1948, May 2011.

[19] J. C. Gomez and M. M. Morcos, "Impact of EV battery chargers on the power quality of distribution systems," *IEEE Transactions on Power Delivery*, vol. 18, pp. 975–981, July 2003.

[20] G. Razeghi, L. Zhang, T. Brown, and S. Samuelsen, "Impacts of plug-in hybrid electric vehicles on a residential transformer using stochastic and empirical analysis," *Journal of Power Sources*, vol. 252, pp. 277–285, Apr. 2014.

[21] C. Jiang, R. Torquato, D. Salles, and W. Xu, "Method to Assess the Power-Quality Impact of Plug-in Electric Vehicles," *IEEE Transactions on Power Delivery*, vol. 29, pp. 958–965, Apr. 2014.

[22] R. C. Leou, C. L. Su, and C. N. Lu, "Stochastic Analyses of Electric Vehicle Charging Impacts on Distribution Network," *IEEE Transactions on Power Systems*, vol. 29, pp. 1055–1063, May 2014.

[23] C. H. Tie, C. K. Gan, and K. A. Ibrahim, "The impact of electric vehicle charging on a residential low voltage distribution network in Malaysia," in *2014 IEEE Innovative Smart Grid Technologies - Asia (ISGT ASIA)*, pp. 272–277, May 2014.

[24] J. Kiviluoma and P. Meibom, "Methodology for modelling plug-in electric vehicles in the power system and cost estimates for a system with either smart or dumb electric vehicles," *Energy*, vol. 36, pp. 1758–1767, Mar. 2011.

[25] E. C. Kara, J. S. Macdonald, D. Black, M. Bérges, G. Hug, and S. Kiliccote, "Estimating the benefits of electric vehicle smart charging at non-residential locations: A data-driven approach," *Applied Energy*, vol. 155, pp. 515–525, Oct. 2015.

[26] A. Weis, P. Jaramillo, and J. Michalek, "Estimating the potential of controlled plug-in hybrid electric vehicle charging to reduce operational and capacity expansion costs for electric power systems with high wind penetration," *Applied Energy*, vol. 115, pp. 190–204, Feb. 2014.

[27] M. Leo, *Ancillary Service Revenue Opportunities from Electric Vehicles via Demand Response*. PhD thesis, University of Michigan, 2011.

[28] M. Ansari, A. Al-Awami, E. Sortomme, and M. Abidoeric, "Coordinated Bidding of Ancillary Services for Vehicle-to-Grid Using Fuzzy Optimization," *IEEE Transactions on Smart Grid*, vol. 6, pp. 261–270, Jan. 2015.

[29] Z. Liu, D. Wang, H. Jia, N. Djilali, and W. Zhang, "Aggregation and bidirectional charging power control of plug-in hybrid electric vehicles: Generation system adequacy analysis," *IEEE Transactions on Sustainable Energy*, vol. 6, no. 2, pp. 325–335, 2015.

[30] N. Xu and C. Chung, "Well-being analysis of generating systems considering electric vehicle charging," *IEEE Transactions on Power Systems*, vol. 29, no. 5, pp. 2311–2320, 2014.

[31] N. Xu and C. Chung, "Uncertainties of ev charging and effects on well-being analysis of generating systems," *IEEE Transactions on Power Systems*, vol. 30, no. 5, pp. 2547–2557, 2015.

[32] R. J. Bessa and M. A. Matos, "Optimization models for an EV aggregator selling secondary reserve in the electricity market," *Electric Power Systems Research*, vol. 106, pp. 36–50, Jan. 2014.

[33] C. Goebel and H. A. Jacobsen, "Aggregator-Controlled EV Charging in Pay-as-Bid Reserve Markets With Strict Delivery Constraints," *IEEE Transactions on Power Systems*, vol. 31, pp. 4447–4461, Nov. 2016.

[34] E. Sortomme and M. A. El-Sharkawi, "Optimal Charging Strategies for Unidirectional Vehicle-to-Grid," *IEEE Transactions on Smart Grid*, vol. 2, pp. 131–138, Mar. 2011.

[35] D. Wu, D. C. Aliprantis, and L. Ying, "Load Scheduling and Dispatch for Aggregators of Plug-In Electric Vehicles," *IEEE Transactions on Smart Grid*, vol. 3, pp. 368–376, Mar. 2012.

[36] J. Tan and L. Wang, "A two-layer evolution strategy particle swarm optimization algorithm for plug-in hybrid electric vehicles at residential distribution grid," in *2014 IEEE PES General Meeting — Conference Exposition*, pp. 1–5, July 2014.

[37] J. Tan and L. Wang, "Integration of Plug-in Hybrid Electric Vehicles into Residential Distribution Grid Based on Two-Layer Intelligent Optimization," *IEEE Transactions on Smart Grid*, vol. 5, pp. 1774–1784, July 2014.

[38] E. Sortomme and M. A. El-Sharkawi, "Optimal Scheduling of Vehicle-to-Grid Energy and Ancillary Services," *IEEE Transactions on Smart Grid*, vol. 3, pp. 351–359, Mar. 2012.

[39] M. E. Khodayar, L. Wu, and M. Shahidehpour, "Hourly Coordination of Electric Vehicle Operation and Volatile Wind Power Generation in SCUC," *IEEE Transactions on Smart Grid*, vol. 3, pp. 1271–1279, Sept. 2012.

[40] C. Jin, J. Tang, and P. Ghosh, "Optimizing Electric Vehicle Charging With Energy Storage in the Electricity Market," *IEEE Transactions on Smart Grid*, vol. 4, pp. 311–320, Mar. 2013.

[41] J. Tan and L. Wang, "A Game-Theoretic Framework for Vehicle-to-Grid Frequency Regulation Considering Smart Charging Mechanism," *IEEE Transactions on Smart Grid*, vol. PP, no. 99, pp. 1–12, 2016.

[42] J. Tan and L. Wang, "Coordinated optimization of PHEVs for frequency regulation capacity bids using hierarchical game," in *Power & Energy Society General Meeting, 2015 IEEE*, pp. 1–5, IEEE, 2015.

[43] Z. Ma, D. Callaway, and I. Hiskens, "Decentralized charging control for large populations of plug-in electric vehicles: Application of the Nash certainty equivalence principle," in *2010 IEEE International Conference on Control Applications*, pp. 191–195, Sept. 2010.

[44] L. Gan, U. Topcu, and S. H. Low, "Optimal decentralized protocol for electric vehicle charging," *IEEE Transactions on Power Systems*, vol. 28, pp. 940–951, May 2013.

[45] C. K. Wen, J. C. Chen, J. H. Teng, and P. Ting, "Decentralized Plug-in Electric Vehicle Charging Selection Algorithm in Power Systems," *IEEE Transactions on Smart Grid*, vol. 3, pp. 1779–1789, Dec. 2012.

[46] Y. Cao, S. Tang, C. Li, P. Zhang, Y. Tan, Z. Zhang, and J. Li, "An Optimized EV Charging Model Considering TOU Price and SOC Curve," *IEEE Transactions on Smart Grid*, vol. 3, pp. 388–393, Mar. 2012.

[47] E. Xydas, C. Marmaras, and L. M. Cipcigan, "A multi-agent based scheduling algorithm for adaptive electric vehicles charging," *Applied Energy*, vol. 177, pp. 354–365, Sept. 2016.

[48] E. L. Karfopoulos and N. D. Hatziargyriou, "A Multi-Agent System for Controlled Charging of a Large Population of Electric Vehicles," *IEEE Transactions on Power Systems*, vol. 28, pp. 1196–1204, May 2013.

[49] T. Logenthiran and D. Srinivasan, "Multi-agent system for managing a power distribution system with Plug-in Hybrid Electrical vehicles in smart grid," in *Innovative Smart Grid Technologies - India (ISGT India), 2011 IEEE PES*, pp. 346–351, Dec. 2011.

[50] C. Wu, H. Mohsenian-Rad, and J. Huang, "Vehicle-to-Aggregator Interaction Game," *IEEE Transactions on Smart Grid*, vol. 3, pp. 434–442, Mar. 2012.

[51] Z. Fan, "A Distributed Demand Response Algorithm and Its Application to PHEV Charging in Smart Grids," *IEEE Transactions on Smart Grid*, vol. 3, pp. 1280–1290, Sept. 2012.

[52] Y. Ota, H. Taniguchi, T. Nakajima, K. M. Liyanage, J. Baba, and A. Yokoyama, "Autonomous Distributed V2G (Vehicle-to-Grid) Satisfying Scheduled Charging," *IEEE Transactions on Smart Grid*, vol. 3, pp. 559–564, Mar. 2012.

[53] Y. He, B. Venkatesh, and L. Guan, "Optimal Scheduling for Charging and Discharging of Electric Vehicles," *IEEE Transactions on Smart Grid*, vol. 3, pp. 1095–1105, Sept. 2012.

[54] N. ISO, "Alternate route: Electrifying the transportation sector," *New York ISO, NY, Tech. Report, June*, 2009.

[55] "U.S. Department of Transportation, Federal Highway Administration, 2009 National Household Travel Survey." `http://nhts.ornl.gov/`.

[56] I. Rahman, P. M. Vasant, B. S. M. Singh, M. Abdullah-Al-Wadud, and N. Adnan, "Review of recent trends in optimization techniques for plug-in hybrid, and electric vehicle charging infrastructures," *Renewable and Sustainable Energy Reviews*, vol. 58, pp. 1039–1047, 2016.

[57] M. Yilmaz and P. T. Krein, "Review of battery charger topologies, charging power levels, and infrastructure for plug-in electric and hybrid vehicles," *IEEE Transactions on Power Electronics*, vol. 28, no. 5, pp. 2151–2169, 2013.

[58] S. Mirjalili and S. Z. M. Hashim, "A new hybrid psogsa algorithm for function optimization," in *Computer and information application (ICCIA), 2010 international conference on*, pp. 374–377, IEEE, 2010.

[59] C. Zhou, K. Qian, M. Allan, and W. Zhou, "Modeling of the cost of ev battery wear due to v2g application in power systems," *IEEE Transactions on Energy Conversion*, vol. 26, no. 4, pp. 1041–1050, 2011.

[60] W. Kempton and J. Tomić, "Vehicle-to-grid power fundamentals: Calculating capacity and net revenue," *Journal of power sources*, vol. 144, no. 1, pp. 268–279, 2005.

[61] W. Su, H. Eichi, W. Zeng, and M.-Y. Chow, "A survey on the electrification of transportation in a smart grid environment," *IEEE Transactions on Industrial Informatics*, vol. 8, no. 1, pp. 1–10, 2012.

[62] M. Bhavaraju, R. Billinton, R. Brown, J. Endrenyi, W. Li, A. Meliopoulos, and C. Singh, "Ieee tutorial on electric delivery system reliability evaluation," in *IEEE Power Engineering Society General Meeting*, 2005.

[63] R. Billinton, *Reliability Evaluation of Power Systems*. Springer Science & Business Media, 2013.

[64] L. Anstine, R. Burke, J. Casey, R. Holgate, R. John, and H. Stewart, "Application of probability methods to the determination of spinning reserve requirements for the pennsylvania-new jersey-maryland interconnection," *IEEE Transactions on Power Apparatus and Systems*, vol. 82, no. 68, pp. 726–735, 1963.

[65] C. L. Borges, D. M. Falcao, J. C. O. Mello, and A. C. Melo, "Composite reliability evaluation by sequential monte carlo simulation on parallel and distributed processing environments," *IEEE Transactions on Power Systems*, vol. 16, no. 2, pp. 203–209, 2001.

[66] F. F. C. Véliz, C. L. T. Borges, and A. M. Rei, "A comparison of load models for composite reliability evaluation by nonsequential monte carlo simulation," *IEEE Transactions on Power Systems*, vol. 25, no. 2, pp. 649–656, 2010.

[67] R. Billinton, S. Kumar, N. Chowdhury, K. Chu, K. Debnath, L. Goel, E. Khan, P. Kos, G. Nourbakhsh, and J. Oteng-Adjei, "A reliability test system for educational purposes-basic data," *IEEE Transactions on Power Systems*, vol. 4, no. 3, pp. 1238–1244, 1989.

[68] C. Grigg, P. Wong, P. Albrecht, R. Allan, M. Bhavaraju, R. Billinton, Q. Chen, C. Fong, S. Haddad, S. Kuruganty, *et al.*, "The ieee reliability test system-1996. a report prepared by the reliability test system task force of the application of probability methods subcommittee," *IEEE Transactions on power systems*, vol. 14, no. 3, pp. 1010–1020, 1999.

[69] E. Ela, M. R. Milligan, and B. Kirby, *Operating Reserves and Variable Generation: A comprehensive review of current strategies, studies, and fundamental research on the impact that increased penetration of variable renewable generation has on power system operating reserves.* National Renewable Energy Laboratory, 2011.

[70] H. Nosair and F. Bouffard, "Reconstructing operating reserve: Flexibility for sustainable power systems," *IEEE Transactions on Sustainable Energy*, vol. 6, no. 4, pp. 1624–1637, 2015.

[71] A. van Stiphout, K. De Vos, and G. Deconinck, "The impact of operating reserves on investment planning of renewable power systems," *IEEE Transactions on Power Systems*, vol. 32, no. 1, pp. 378–388, 2017.

[72] L. Wu, M. Shahidehpour, and T. Li, "Cost of reliability analysis based on stochastic unit commitment," *IEEE Transactions on Power Systems*, vol. 23, no. 3, pp. 1364–1374, 2008.

[73] C. Chen and S. Che, "Short-term unit commitment with simplified economic dispatch," *Electric Power Systems Research*, vol. 21, no. 2, pp. 115–120, 1991.

[74] C.-L. Chen, "Optimal wind–thermal generating unit commitment," *IEEE transactions on energy conversion*, vol. 23, no. 1, pp. 273–280, 2008.

[75] R. Billinton and A. V. Jain, "The effect of rapid start and hot reserve units in spinning reserve studies," *IEEE Transactions on Power Apparatus and Systems*, no. 2, pp. 511–516, 1972.